Sexual antagonism, mating systems, and recombination suppression on sex chromosomes

Ewan Flintham[1,*] and Charles Mullon[1]

[1]Department of Ecology and Evolution, University of Lausanne, 1015 Lausanne, Switzerland

[*]Correspondence: ewan.flintham@unil.ch

Abstract. The suppression of recombination between sex chromosomes is a widespread feature of genetic sex determination systems. Such recombination arrest is thought to trigger sex chromosome divergence and degeneration and has evolved multiple times in homomorphic ancestors, making it a striking case of convergent evolution. Existing models for the evolution of recombination suppression fall into two main categories: those that rely on the prior segregation of sexually-antagonistic alleles and those that do not. Using mathematical modelling, we compare here the tempo of recombination evolution via the fixation of neutral recombination suppressors with those capturing a locus contributing to a sexually antagonistic trait. We do this for a trait locus with fixed effects and for a locus where allelic effects evolve. We show that sexual antagonism significantly accelerates the substitution of recombination modifiers relative to genetic drift alone, though the strength of this effect depends on the nature of sexually antagonistic variation and on the mating system. Where allelic values at the trait locus evolve, sexually antagonistic selection leads to a pattern of male heterozygote advantage that results in especially rapid substitution by recombination modifiers. We also find that recombination suppression driven by sexual antagonism often arises on the homogametic chromosome, which is not the case when suppression evolves solely due to drift. This pattern is especially strong in XY systems where male reproductive success is highly variable. Our results highlight sexual antagonism as a key driver of recombination arrest, and suggest that reproductive ecology may play a previously underappreciated role in the evolution and stability of sex chromosome systems.

1 Introduction

In many species with separate sexes, an individual's sex is determined by its karyotype, in particular the identity of its sex chromosomes (Bachtrog et al., 2014). These chromosomes contain the genes that instigate sex-specific development, which are held together in a genomic region that does not recombine in at least one sex (a sex-determining region, or "SDR", Otto et al., 2011; Wright et al., 2016). For example in XY species, sex is assigned according to the presence or absence of a dominant male-determining locus on the Y-chromosome, around which recombination is suppressed in males. This situation is mirrored in ZW species, where a dominant female-determining factor sits on the W-chromosome, leading to recombination suppression in females. Strong genetic linkage between sex-determining loci in the heterogametic sex is thought to be adaptive as it ensure alleles responsible for sexual development are co-inherited (Charlesworth and Charlesworth, 2005; Nei, 1969). However, regions of suppressed recombination that extend well beyond the vicinity of sex-determining loci, often encompassing the majority or even entirety of the chromosome, have evolved independently in many species (Bachtrog et al., 2014; Bergero and Charlesworth, 2009). Extensive recombination suppression in the heterogematic sex is considered a hallmark of a sex chromosome system (Otto, 2014).

The classical explanation for the evolution of recombination suppression along sex chromosomes is that it is favoured by selection because it ensures the co-inheritance of a sex-determining factor with alleles that are beneficial when expressed in that sex (i.e., that contribute to sex-specific adaptation, Beukeboom and Perrin, 2014; Fisher, 1931; Ponnikas et al., 2018; Wright et al., 2016). Theoretical population genetic models have been integral to our understanding of this process. Early models showed that selection favours the invasion of a Y-linked recombination suppressor if it captures a male SDR and the male-beneficial allele at a sexually antagonistic locus under balancing selection (which was modelled as a single di-allelic site with fixed fitness effects; Charlesworth and Charlesworth, 1980; Nei, 1969). Lenormand (2003) further showed that a modifier decreasing recombination by a small amount would be favoured if it increased linkage between the SDR and a polymorphic locus experiencing sex-specific selection – although without balancing selection variation at such a locus would be weak, limiting the scope for selection on recombination. This result was then found to hold for most levels of linkage between a modifier, the SDR and a locus under selection (Otto, 2014). Finally, Olito and Abbott (2023) and Olito et al. (2024) estimated the invasion probability for an inversion linking a Y-linked SDR with a di-allelic sexually antagonistic locus with weak fitness effects in a large

well-mixed population, and used this to make predictions about the chromosomal length that should be affected by recombination suppression.

In contrast to the classic sexual antagonism explanation, a more recent group of models show it is possible for recombination suppression on sex chromosomes to evolve without sex-specific selection (reviewed in Charlesworth and Olito, 2024; Jay et al., 2024; Olito and Abbott, 2023; Ponnikas et al., 2018). Here, recombination suppressors capture the SDR and a nearby region of the chromosome that is either (i) neutral (i.e., contains no segregating loci affecting fitness; Charlesworth and Charlesworth, 2005; Ironside, 2010) and then fixes by chance owing to genetic drift; or (ii) includes loci at which deleterious recessive variants segregate in the population. In this second case, a "lucky" suppressor mutant that happens to appear in a particularly unloaded background (i.e., captures a set of loci at which fewer than average deleterious alleles are present; Ironside, 2010; Jay et al., 2022; Lenormand and Roze, 2022), experiences a transient fitness advantage that helps drive its fixation (although it has been argued that for most of biologically plausible parameter space this effect does not appreciably increase the invasion probability of a suppressor compared to neutrality, implying that neutral and lucky suppressors may have similar impacts on sex chromosome evolution; Charlesworth and Olito, 2024; Olito and Abbott, 2023; Olito et al., 2024). In both scenarios, recombination arrest must later be stabilised in the face of mutations that restore recombination (e.g., reversions; Lenormand and Roze, 2024). This may occur through the development of structural incompatibilities between sex chromosome homologues after recombination arrest (Jay et al., 2024), or through sex-specific divergence in gene regulation at loci within the non-recombining region, leading to low fitness recombinants (Lenormand and Roze, 2022).

While theory has demonstrated that sexual antagonism and the chance fixation of neutral or lucky suppressors can in principle drive recombination arrest, the relative contribution of these processes to sex chromosome evolution remains an open question (Jay et al., 2024; Lenormand and Roze, 2024; Olito and Abbott, 2023; Ponnikas et al., 2018). In particular, it is unclear whether the fixation of suppressors due to sexually antagonistic selection or genetic drift occurs on comparable timescales or not. Evaluating this, however, is not straightforward. This is because rates of substitution for recombination modifiers are sensitive to multiple factors, such as the nature and availability of segregating sexually antagonistic variation, the mating system (which influences the degree of genetic drift experienced by different parts of the genome; Laporte and Charlesworth, 2002), and the potential for recombination suppressors to arise in different sex-linked genomic regions.

Here, we address some of these issues by relaxing a number of assumptions common to prior mod-

els. First, instead of assuming that sexually-antagonistic loci are di-allelic with (typically weak) fixed selection coefficients (e.g., Charlesworth and Charlesworth, 1980; Lenormand, 2003; Nei, 1969; Olito and Abbott, 2023), we assume allelic effects contribute to a quantitative trait under sex-specific selection of arbitrary strength, and allow them to evolve through time. Second, we relax the assumption that reproduction occurs through the random-union-of-gametes (as assumed under a Wright-Fisher sampling process), which leads to equal reproductive variance in males and females. In particular, we allow for a polygynous mating system, common to many species experiencing sex-specific selection (Bonduriansky and Chenoweth, 2009), that leads to stronger reproductive variance in males. Third, we investigate the possibility for suppressors of recombination to accumulate on the homogametic sex chromosome (X or Z chromosome) rather than just the heterogametic one (Y or W), as is assumed in many models (e.g., Charlesworth and Charlesworth, 1980; Lenormand and Roze, 2022; Nei, 1969; Olito and Abbott, 2023).

2 Model

2.1 Lifecycle and fitness

We consider a diploid population of large and constant size N, composed of equal numbers of adult males and females, with non-overlapping generations. Males and females reproduce to generate zygotes that become male and female juveniles with equal probability (i.e. the sex ratio at birth is unbiased). Adults die and juveniles compete sex-specifically to become the male and female adults of the next generation. As a baseline, we assume that reproduction occurs through the random union of male and female gametes but account later for explicit mating amongst males and females, such that males may show stronger reproductive variance than females.

Each individual expresses a quantitative trait z that influences its reproductive success in a sex-specific manner. We denote male and female fecundity by $w_{\mathrm{m}}(z)$ and $w_{\mathrm{f}}(z)$ respectively. Unless otherwise stated, we assume that these are given by Gaussian functions: $w_{\mathrm{m}}(z) \propto e^{-\sigma_{\mathrm{m}}(1+z)^2}$ and $w_{\mathrm{f}}(z) \propto e^{-\sigma_{\mathrm{f}}(1-z)^2}$ (as in e.g. Connallon and Clark, 2014a,b; Fisher, 1958; Flintham et al., 2024; Lande, 1980; Muralidhar and Coop, 2023), such that male fitness is maximised by trait value $z = -1$ and female fitness by $z = 1$, where σ_{m} and σ_{f} determine how steeply fitness declines with the difference between the trait value of an individual and the optimum in males and females respectively (i.e. σ_{m} and σ_{f} modulate the strength of selection in males and females).

2.2 Evolutionary dynamics at the trait locus

We assume z is influenced by a locus ("trait locus" or "z-locus") in the pseudo-autosomal region (PAR) of a sex chromosome that is recombining with a male SDR with a probability $r > 0$ per meiosis (for illustrative purposes we are therefore considering an XY system, but our model also applies to ZW species, see section 4.2 for discussion). Alleles at this locus have additive effects on phenotype, such that an individual's trait value is given by $z = x_1 + x_2$ where x_1 is the allelic value carried on its maternally inherited X-chromosome and x_2 is the allelic value carried on its paternally inherited chromosome (which is an X-chromosome in females and a Y-chromosome in males). Allelic effects at the trait locus evolve according to Kimura's continuum-of-alleles model (Kimura, 1965): when they occur, mutations add a small random deviation with mean zero onto the existing allelic value of the mutated allele (we also consider the case where allelic values have evolved through arbitrarily sized mutations, as in classical population genetic models of sexual antagonism; Haldane, 1962; Kidwell et al., 1977; Rice, 1984, see section 2.3).

2.2.1 Emergence of polymorphism

Provided mutations are sufficiently rare compared to selection, evolution occurs in two phases under our assumptions (see Flintham et al., 2024 for a detailed description of the gradual evolutionary dynamics on the PAR under the continuum-of-alleles model; Appendix A.1 here for derivation). First, the population evolves under directional selection through a series of substitutions whereby positively selected mutations rapidly sweep to fixation such that the population "jumps" from one trait value to another. Eventually the population converges to the equilibrium trait value

$$z^* = 2x^* = \frac{\sigma_\mathrm{f} - \sigma_\mathrm{m}}{\sigma_\mathrm{f} + \sigma_\mathrm{m}}, \tag{1}$$

which is independent of the recombination rate r (this equilibrium is therefore equivalent to the equilibrium trait value that would be produced by gradual evolution if z were encoded by an autosomally encoded locus, i.e., where $r = 0.5$). When selection is equally strong in both sexes ($\sigma_\mathrm{m} = \sigma_\mathrm{f}$), the trait equilibrium is equidistant from the male and female optima ($z^* = x^* = 0$), otherwise it is closer to the optimum of the sex where selection is stronger.

Once the population expresses z^*, selection is then either stabilising, such that allelic values remain distributed around x^* under mutation-selection balance; or disruptive whereby their distribution

becomes bimodal in a process referred to as "evolutionary branching" leading to the maintenance of a polymorphism under balancing selection (Dercole and Rinaldi, 2008; Geritz et al., 1998; Rueffler et al., 2006). Here, evolutionary branching occurs when

$$r < \frac{8\sigma_{\mathrm{m}}^2\sigma_{\mathrm{f}}^2}{(\sigma_{\mathrm{m}}+\sigma_{\mathrm{f}})^3} \tag{2}$$

(see eq. B-25 in Flintham et al., 2024 for condition with general male and female fitness functions). Eq. (2) is satisfied most easily when σ_{m} and σ_{f} are large and similar, with the most permissive condition occurring when selection is equally strong in both sexes ($\sigma = \sigma_{\mathrm{m}} = \sigma_{\mathrm{f}}$), at which point eq. (2) simplifies to $r < \sigma$. Thus polymorphism occurs most readily at loci encoding traits under strong and symmetrical sexually antagonistic selection (σ large) or those close to the SDR-PAR boundary (r small). This is because linkage with the SDR facilitates an association between a sexually antagonistic allele and carriage in the sex it benefits; an association that strongly favours polymorphism (Avila and Mullon, 2023; Charlesworth et al., 2014; Flintham et al., 2024; Jordan and Charlesworth, 2012).

2.2.2 Balancing selection and divergence

After evolutionary branching has occurred, balancing selection maintains two alleles, which we denote A and a. These two alleles initially encode weakly differentiated allelic values around x^* (x_{A} and x_{a}, respectively) but these values become increasingly divergent as the two alleles accumulate further mutations (Geritz and Kisdi, 2000). Without loss of generality, we assume that allele A is favoured by females while allele a is favoured by males (such that $x_{\mathrm{A}} > x^*$ and $x_{\mathrm{a}} < x^*$).

Evolutionary divergence between the female and male beneficial alleles can be characterised from the invasion fitness (or geometric growth rate), $W(x_\bullet, x_{\mathrm{A}}, x_{\mathrm{a}})$, of a rare mutant allele that encodes $x_\bullet$ in a population where alleles A and a are at equilibrium owing to balancing selection. Divergence between the female and male beneficial alleles continues until directional selection on both allelic values ceases (i.e. where allelic values x_{A}^* and x_{a}^* are such that $s_{\mathrm{A}}(x_{\mathrm{A}}^*, x_{\mathrm{a}}^*) = s_{\mathrm{a}}(x_{\mathrm{A}}^*, x_{\mathrm{a}}^*) = 0$, where $s_{\mathrm{A}}(x_{\mathrm{A}}, x_{\mathrm{a}}) = \partial W(x_\bullet, x_{\mathrm{A}}, x_{\mathrm{a}})/\partial x_\bullet|_{x_\bullet = x_{\mathrm{A}}}$ and $s_{\mathrm{a}}(x_{\mathrm{A}}, x_{\mathrm{a}}) = \partial W(x_\bullet, x_{\mathrm{A}}, x_{\mathrm{a}})/\partial x_\bullet|_{x_\bullet = x_{\mathrm{a}}}$). The population then remains polymorphic for alleles A and a, respectively with allelic effect x_{A}^* and x_{a}^*. Our characterisation of this process is detailed in Appendix A.2, and a simulated example is shown in Fig. 1A.

The allelic coalition $(x_{\mathrm{a}}^*, x_{\mathrm{A}}^*)$ represents the long-term outcome of stable sexually antagonistic selec-

tion, i.e., constant sex-specific selection and constraints on genetic architecture that prevent the evolution of sex-specific gene expression (Bonduriansky and Chenoweth, 2009). We discuss the interpretation of x_a^* and x_A^*, and their implications for segregating variation under different models of mutation in section 4.1.

2.3 Invasion of a recombination suppressor

The main aim of our study is to investigate the fate of a new mutation contained within the PAR that fully suppresses recombination between the SDR and the z-locus (such as an inversion that captures both regions). We initially assume this mutation appears on the Y-chromosome (is Y-linked) and captures the SDR itself, but in section 3.4 we consider a suppressor appearing on the X-chromosome (i.e., in X-linkage), and captures the homologous genomic region to the SDR on the X. These recombination modifiers are assumed to arise in a population that is polymorphic at the z-locus. As a basis to our analyses, we use the invasion fitness $W_r^Y(x_a, x_A)$ of a rare Y-linked suppressor in a population where recombination occurs at rate r and where alleles with effect sizes x_a and x_A segregate at their equilibrium frequencies (Appendix B.1 for our characterization of $W_r^Y(x_a, x_A)$). Throughout, we consider two cases: (1) where alleles A and a have diverged to their evolutionary equilibrium (i.e., $x_A = x_A^*$ and $x_a = x_a^*$), as would occur if mutations at recombination modifiers within the PAR occur more rarely than those influencing allelic effects at the trait locus; and (2) where divergence is ongoing, or where A and a have diverged through a recent large effect mutation (i.e., we consider arbitrary allelic effects $x_A < x_a$ that generate a balanced polymorphism for a and A).

3 Results

3.1 Sexually antagonistic polymorphism on the PAR generates male heterozygote advantage

As a first step, we characterise the polymorphism that evolves at the trait locus whilst keeping recombination rate fixed at r. Using a numerical approach (Appendix A.2, in particular Appendix A.2.3) we find that for all parameters considered (such that condition (2) holds), the equilibrium allelic coalition always consists of two alleles – a and A – that respectively encode trait values x_a^* and x_A^* such that: (i) in females, aa homozygotes show the greatest fitness; (ii) in males, Aa heterozygotes show the

greatest fitness (Fig. 1A-B for an example, and see Fig. 1C and SI Fig. 1 for x_a^* and x_A^* across a broad range of parameter sets). This occurs because one allele, a here, leads homozygotes to express a trait value close to the female optimum, while the other allele A leads homozygotes to express a trait value further from the male optimum than the one expressed by Aa heterozygotes (which occurs whenever $x_A < -(2 + x_a)/3$).

The "overshooting" of the male trait optimum by allele A occurs because once both alleles have begun diverging, Aa is the most frequent male genotype and hence selection on A favours these heterozygotes to be best adapted, at the expense of AA males. To see why, consider that once two alleles have diverged in their phenotypic effects, selection leads male-beneficial allele A to become overrepresented in the Y-chromosome and thus Y-bearing sperm, while female-beneficial allele a becomes overrepresented in X-bearing eggs. This generates an increase in the number of female (XX) offspring that are aa homozygote, and an increase the number of male (XY) offspring that are Aa heterozygotes (meanwhile, the number of offspring that are AA homozygotes decreases, owing to the low frequency of A in eggs). Consequently, selection favours an allelic value x_A for A that is greater than the male optimum in homozygotes because this x_A confers high male fitness in heterozygotes when combined with an allelic value x_a that confers high female fitness in homozygotic form (e.g., with $\sigma_m = \sigma_f$, the combination of allelic values $x_A = -1.5$ and $x_a = 0.5$ on average encode the fittest phenotypes as they satisfy $x_A + x_a = -1$, the male optimum, and $x_a + x_a = 1$, the female optimum).

3.2 Sexual antagonism favours recombination suppression, especially with evolutionarily stable polymorphism

Next, we consider the fate of a recombination modifier on the Y-chromosome that arises as a single copy and fully suppresses recombination between the SDR and the trait locus. We initially consider the trait locus to be polymorphic for two alleles A and a with arbitrary allelic values x_A and x_a, and later focus on the case where they have evolved to their evolutionary equilibrium x_A^* and x_a^*. We show that a Y-linked suppressor of recombination can invade due to selection only if it captures the male-beneficial allele A (where $x_A < x^* < x_a$), in which case its invasion fitness reads as

$$W_r^Y(x_a, x_A) = \frac{w_m(x_a + x_A)(1 - \hat{p}_f) + w_m(2x_A)\hat{p}_f}{(1 - \hat{p}_m^Y)(1 - \hat{p}_f)\, w_m(2x_a) + \hat{p}_m^Y \hat{p}_f w_m(2x_A) + (\hat{p}_m^Y + \hat{p}_f - 2\hat{p}_m^Y \hat{p}_f)\, w_m(x_a + x_A)}, \tag{3}$$

where $\hat{p}_f$ and $\hat{p}_m^Y$ denote the equilibrium gametic frequencies of A in eggs and Y-bearing sperm, respectively (Appendix B.1 for derivation; see Olito and Abbott, 2023 their Appendix C eq. 15 for equiva-

lent expression for a di-allelic sexually antagonistic locus with fixed effects, and Otto, 2014 for expressions for a small effect recombination modifier). Although the resident recombination rate r does not appear explicitly in eq. (3), r does influence $W_r^{\mathrm{Y}}(x_{\mathrm{a}}, x_{\mathrm{A}})$ indirectly because the equilibrium frequencies of A depend on it (i.e., $\widehat{p}_{\mathrm{f}}$ and $\widehat{p}_{\mathrm{m}}^{\mathrm{Y}}$ depend on r, x_{A} and x_{A}; Appendix B.1 for details).

A recombination suppressor is favoured by selection if $W_r^{\mathrm{Y}}(x_{\mathrm{a}}, x_{\mathrm{A}}) > 1$, which upon rearranging eq. (3), we find can occur via two routes: either

$$\begin{cases} w_{\mathrm{m}}(2x_{\mathrm{A}}) > w_{\mathrm{m}}(x_{\mathrm{A}} + x_{\mathrm{a}}), & \text{(4a)} \\ \text{or} & \\ \widehat{p}_{\mathrm{f}} < \dfrac{w_{\mathrm{m}}(x_{\mathrm{a}} + x_{\mathrm{A}}) - w_{\mathrm{m}}(2x_{\mathrm{a}})}{2w_{\mathrm{m}}(x_{\mathrm{a}} + x_{\mathrm{A}}) - w_{\mathrm{m}}(2x_{\mathrm{a}}) - w_{\mathrm{m}}(2x_{\mathrm{A}})}. & \text{(4b)} \end{cases}$$

The first route (eq. 4a) is for the homozygote AA to encode the highest fitness in males (i.e. $w_{\mathrm{m}}(2x_{\mathrm{A}}) > w_{\mathrm{m}}(x_{\mathrm{A}} + x_{\mathrm{a}})$), whereas the second route (eq. 4b) applies if instead the heterozygote Aa encodes the highest fitness (i.e. $w_{\mathrm{m}}(x_{\mathrm{A}} + x_{\mathrm{a}}) > w_{\mathrm{m}}(2x_{\mathrm{A}})$ such that males exhibit heterozygote advantage). The increased certainty in the patrilineal transmission of allele A brought by recombination suppression is advantageous if either: (a) this allele A is systematically male-beneficial such that AA homozygotes enjoy the greatest male fitness (as in condition 4a); or (b) males show heterozygote advantage and the frequency $\widehat{p}_{\mathrm{f}}$ of allele A amongst eggs is sufficiently low such that a male always passing on A through his Y-chromosome produces male offspring that are mostly Aa heterozygotes (hence condition 4b being more stringent when $\widehat{p}_{\mathrm{f}}$ is large).

To gain more quantitative insights, we computed $W_r^{\mathrm{Y}}(x_{\mathrm{a}}, x_{\mathrm{A}})$ for a wide range of parameters, varying allelic values x_{a} and x_{A}, the strengths of selection σ_{m} and σ_{f}, and resident recombination rate r (solving for equilibrium allele frequencies $\widehat{p}_{\mathrm{f}}$ and $\widehat{p}_{\mathrm{m}}^{\mathrm{Y}}$ numerically; Appendix B.1 for details). This shows that provided a and A are maintained by balancing selection in the resident population, selection always favours a full recombination suppressor, i.e., $W_r^{\mathrm{Y}}(x_{\mathrm{a}}, x_{\mathrm{A}}) > 1$ (as known to be the case for a small effect recombination modifier; Otto, 2014, see her condition for selection to favour suppression with $R_m = 0$). For weakly diverged alleles (x_{a} and x_{A} similar), this is simply because condition (4a) is always satisfied when a and A segregate. For alleles that generate male heterozygote advantage, this tells us that under conditions leading to balancing selection on the PAR, recombination and sexually antagonistic selection always drive sufficiently low frequencies $\widehat{p}_{\mathrm{f}}$ of allele A in eggs to satisfy condition (4b).

Our results also indicate that the strength of selection on suppression is sensitive to the strength of recombination in the resident population, with $W_r^{\mathrm{Y}}(x_{\mathrm{a}}, x_{\mathrm{A}})$ being substantially greater when r is large

(compare Figs. 2A-C; see also Olito and Abbott, 2023). This is because when r is small, the frequency $\hat{p}_{\mathrm{m}}^{\mathrm{Y}}$ of A in Y-bearing sperm is high anyway, which diminishes the benefit to a mutant male that ceases recombination.

Selection for recombination suppression is especially strong when alleles have evolved to their evolutionary equilibrium (i.e. $W_r^{\mathrm{Y}}(x_{\mathrm{a}}, x_{\mathrm{A}})$ is especially large when $x_{\mathrm{a}} = x_{\mathrm{a}}^*$ and $x_{\mathrm{A}} = x_{\mathrm{A}}^*$, Figs. 2A-C, white stars). This is due to two complementary effects. First, the equilibrium values x_{a}^* and x_{A}^* entail a large variance in male fitness under random mating, owing to their substantial divergence (in general, selection for recombination suppression increases with the divergence between x_{a} and x_{A}, and so is greatest under the conditions leading to male heterozygote advantage, Fig. 2). Thus, with equilibrium allelic values, Aa males experience an especially large relative fitness advantage over homozygote genotypes, which in turn leads a strong fitness benefit to be conferred by a recombination suppressor that ensures a male's sons inherit A on their Y-chromosome. Second, the equilibrium value x_{a}^* generates the strongest possible positive selection on allele a through females (due to strong homozygote aa advantage), and so leads to the lowest equilibrium frequencies of allele A on the X-chromosome (i.e., low values of $\hat{p}_{\mathrm{f}}$ and $\hat{p}_{\mathrm{m}}^{\mathrm{X}}$). This means resident males on average carry an excess of allele a via their maternal X, and so depart more frequently from the male optimum, reinforcing the competitive advantage of males that carry allele A on their Y-chromosome.

3.3 Sexual antagonism expedites sex chromosome evolution, but its potency is sensitive to the mating system

Our analyses of eq. (3) align with the idea that sexual antagonism generates a fitness benefit to Y-linked recombination suppressor capturing a male-beneficial allele (as in Charlesworth and Charlesworth, 1980; Lenormand, 2003; Nei, 1969; Olito and Abbott, 2023). However, the tempo of recombination evolution depends not just on whether selection can favour a rare suppressor, but also the likelihood such a mutant evades stochastic loss and goes on to fix in the population. To quantify this, we first calculate the (unconditional) probability of invasion Ψ^{Y} of a Y-linked suppressor: the probability that a suppressor arises in a chromosome carrying allele A and that this suppressor does not go extinct in the long run, i.e. $\Psi^{\mathrm{Y}} = \hat{p}_{\mathrm{m}}^{\mathrm{Y}} \Psi_{\mathrm{A}}^{\mathrm{Y}}$, where $\Psi_{\mathrm{A}}^{\mathrm{Y}}$ is the invasion probability of the suppressor conditional on it capturing A and recall $\hat{p}_{\mathrm{m}}^{\mathrm{Y}}$ is the frequency of A in sperm (see Appendix B.2.1 for details, and also Olito and Abbott, 2023 for a similar approach). We show in Appendix B.2.2, that suppressors that do not go extinct (i.e, successfully invade) always go on to fix in the population;

in other words, suppressors never form balanced polymorphisms. The probability of invasion, Ψ^{Y}, is therefore equivalent to the probability of fixation, and this allows us to leverage Ψ^{Y} to compute a suppressor's expected time to substitution, τ (the expected waiting time to arise and then fix in a population, Appendix B.2.2 for details). We use τ as a measure of the rate of recombination evolution.

We first perform this analysis under the life cycle described in section 2.1, where mating is modelled as a random-union-of-gametes model (such that the offspring distribution of a rare recombination suppressor is Poisson with mean given by eq. 3). We calculated Ψ^{Y} for different allelic values x_{a} and x_{A}, and parameters σ_{m}, σ_{f} and r (Appendix B.2.1 for details). As expected from the results of section 3.2, invasion probability Ψ^{Y} is especially large when allelic values are at their evolutionary equilibrium (i.e., when $x_{\mathrm{a}} = x_{\mathrm{a}}^*, x_{\mathrm{A}} = x_{\mathrm{A}}^*$, SI Fig. 3 and Fig. 3A compare dotted and solid lines), and greatest when sexual antagonism is strong and the resident recombination rate is high (σ and r large, Fig. 3A).

More generally, unless allelic values are very weakly diverged (x_{a} and x_{A} similar) or sexually antagonistic selection is very weak (σ very small), Ψ^{Y} is high compared to the neutral expectation in a large population (although not the focus of their paper, this is also visible in Olito and Abbott, 2023 by comparing the scale of Y-axes in Figs. 2A-C). For example, with allelic values $x_{\mathrm{a}} = 0.5$ and $x_{\mathrm{A}} = -0.5$ and loose linkage $r = 0.5$, $\Psi^{\mathrm{Y}} \approx 0.1$ for $\sigma = \sigma_{\mathrm{m}} = \sigma_{\mathrm{f}} = 0.1$ and $\Psi^{\mathrm{Y}} \approx 0.01$ for $\sigma = \sigma_{\mathrm{m}} = \sigma_{\mathrm{f}} = 0.01$ (Fig. 3A). A neutral suppressor would fix with a similar probability only in very small populations (with 10 and 100 males or less for $\sigma = 0.1$ and $\sigma = 0.01$, respectively). In line with this, the expected time to substitution for a recombination suppressor is orders of magnitude shorter if it captures a sexually antagonistic locus than for a neutral suppressor (e.g., with reasonable suppressor mutation rates and $r = 0.5$, a substitution can be expected to occur roughly 1000 times faster than at neutrality when $\sigma = 0.1$, and around 100 times faster when $\sigma = 0.01$, Fig. 3B).

The random-union-of-gametes model is a good approximation for large outbred populations where individuals of both sexes mate many times, but not for the many species experiencing sex-specific reproductive variance or skew (Andersson, 1994; Clutton-Brock and Parker, 1992; Shuker and Simmons, 2014). To capture such a situation, we now consider a lifecycle that begets a lottery polygyny mating system (Lee et al., 2008; Nunney, 1993). Briefly, we assume females mate singly but males can mate multiply (full details of this life cycle are given in Appendix. B.2.3). A male's likelihood of mating each female is determined by his relative mating competitiveness, which is a random value assigned to him upon reaching adulthood (e.g. capturing his biological "condition", Wilson and Nussey, 2010, which we assume is independent of genotype here, in order to facilitate comparison between models). Male reproductive variance therefore emerges because some males mate on average more females, and

this effect can be tuned by modifying the distribution of male mating competitiveness, with variance in mating competitiveness modulating the distribution of male mating and reproductive success (Lee et al., 2008). We detail how we calculate the probability of invasion Ψ^{Y} of a Y-linked suppressor under this model in Appendix B.2.3.

Comparison between Ψ^{Y} calculated under this model and under the random-union-of-gametes reveals that Y-linked recombination suppressors are less likely to invade under lottery polygyny (Fig. 3C). This is because high variability in male mating success elevates the probability that a male by chance mates no females and so produces no offspring. This in turn exacerbates the probability that the lineage carrying a recombination suppressor suffers stochastic extinction. Consequently, adaptive (i.e., those capturing allele A) suppressors will fix with probabilities similar to neutral suppressors in much larger population under lottery polygyny than under the random-of-union-of-gametes model – especially when males show large variability in their mating success. For example, where male mating variance is around 10 (which is well within empirical estimates; Wade and Shuster, 2004 Table 1), population sizes of 10^4 males will yield similar neutral and adaptive fixation probabilities when $r = 0.5$ and $\sigma = 0.01$. Accordingly, adaptive recombination suppression evolves more slowly in the presence of high male reproductive variance (Fig. 3D), and even on the same timescale as neutral suppression if sexual antagonism is sufficiently weak (Fig. 3D, $\sigma = 0.001$).

3.4 Sex chromosome evolution is more readily driven by X- than Y-linked suppressors

As a final step, we investigate the potential for recombination evolution to occur through X- versus Y-linked modifiers. Previous theory overwhelmingly attributes recombination suppression among sex chromosomes to Y-linked suppressors (e.g., Charlesworth and Charlesworth, 1980; Lenormand and Roze, 2022; Nei, 1969; Olito et al., 2024). But divergence between sex chromosomes may just as well be mediated by recombination modifiers fixing on the X (Charlesworth and Charlesworth, 1980, 2005). To study this, we now consider the invasion of a suppressor on the X-chromosome in the presence of different allelic values (x_{a} and x_{A}, including their evolutionary equilibrium x_{a}^* and x_{A}^*) and mating systems (random-union-of-gametes and polygyny models). We assume this modifier fully suppresses recombination in both males and heterozygous females (as per an inversion).

We first calculate the invasion fitness of an X-linked suppressor, $W_r^{\mathrm{X}}(x_{\mathrm{a}}, x_{\mathrm{A}})$ (in Appendix C.1). Analysis of $W_r^{\mathrm{X}}(x_{\mathrm{a}}, x_{\mathrm{A}})$ shows that such a suppressor is favoured (i.e., $W_r^{\mathrm{X}}(x_{\mathrm{a}}, x_{\mathrm{A}}) > 1$) for any parameters σ_{m}, σ_{f} and r, and allelic values x_{a} and x_{A} such that a and A are maintained under balancing selec-

tion, if and only if the suppressor captures female-beneficial allele a. This is because linking allele a to the SDR-homologue on the X-chromosome ensures that males always transmit this allele to their female offspring, who then enjoy higher fitness as a result. As with Y-linked suppression, selection favours an X-linked suppressor most strongly (i.e., $W_r^{\mathrm{X}}(x_{\mathrm{a}}, x_{\mathrm{A}})$ is largest) when recombination in males is frequent (r large), with selection especially strong when alleles are at their equilibrium values (x_{a}^* and x_{A}^*) (SI Fig. 4). Selection therefore readily favours X-linked suppression, but we find it does so less strongly than for suppression on the Y (i.e., $W_r^{\mathrm{X}}(x_{\mathrm{a}}, x_{\mathrm{A}}) < W_r^{\mathrm{Y}}(x_{\mathrm{a}}, x_{\mathrm{A}})$, SI Fig. 5A, consistent with the results of Charlesworth and Charlesworth, 1980 for chromosomal fusions). This is primarily because the X spends 2/3 of its time in females where recombination suppression is inconsequential to offspring fitness (as chromosome segregation in females is random with respect to offspring sex). This dilutes the fitness advantage of X-linked recombination suppressors relative to those on the Y, which are passed strictly through males. An additional penalty to X-linked suppression arises for non-equilibrium allelic values where males do not show heterozygote advantage and thus ubiquitously favour A, as here an X-suppressor capturing allele a will confer decreased fitness when carried in males.

Next we calculate the probability of invasion Ψ^{X} for an X-linked suppressor of recombination and compare it with its Y-linked counterpart Ψ^{Y} (Appendices C.2.1-C.3 for full description of invasion probabilities for X-linked suppressors). Where the offspring distribution of a rare X-linked suppressor is Poisson (as expected under the random-union-of-gametes model), we find that such a suppressor is less likely to invade than a suppressor arising on the Y, i.e. $\Psi^{\mathrm{X}} < \Psi^{\mathrm{Y}}$ (SI Fig. 5B). This is unsurprising given that selection favouring X-linked suppression is weaker (i.e., $W_r^{\mathrm{X}}(x_{\mathrm{a}}, x_{\mathrm{A}}) < W_r^{\mathrm{Y}}(x_{\mathrm{a}}, x_{\mathrm{A}})$).

Nevertheless the discrepancy between X and Y invasion probabilities remains moderate – less than three-fold (SI Fig. 5B) – and can therefore be more-than compensated for by stronger X-linked mutational input. When recombination suppressors arise with equal per-base rates in males and females, new suppressors are three times more likely to arise on the X than Y owing to the X's larger population size. Therefore, the probability that a recombination suppression event (i.e., substitution by a suppressor) is due to a Y- rather than an X-linked modifier is $\rho = \Psi^{\mathrm{Y}}/(\Psi^{\mathrm{Y}} + 3\Psi^{\mathrm{X}})$ (provided suppressors arise rarely). Plugging in our values for Ψ^{Y} and Ψ^{X} into ρ reveals that recombination suppression is in fact equally likely to be X- or Y-linked when sexual antagonism is weak or initial linkage between the SDR and trait locus is tight (i.e., $\rho = 0.5$ when r or σ small, Fig. 4A), but that otherwise X-linked suppression is in fact more probable (e.g., $\rho < 0.5$ with $r = 0.5$ and $\sigma \geq 0.1$ for $x_{\mathrm{a}} = 0.5, x_{\mathrm{A}} = -0.5$ and $x_{\mathrm{a}} = x_{\mathrm{a}}^*, x_{\mathrm{A}} = x_{\mathrm{A}}^*$,Fig. 4A).

Computing ρ under lottery polygyny shows that recombination suppression is even more likely to be a consequence of X-linked suppressors with this mating system (Fig. 4B). In particular, when male reproductive variance is high, recombination arrest among sex chromosome is expected to be almost always due to X-linked factors (e.g. with a variance in the number of mates among males of around 10, $\rho \approx 0.1$, Fig. 4B). This is because male reproductive variance has less influence on the level of drift experienced by X- than Y-linked mutations so that, all else equal, X-linked suppressors are less susceptible to stochastic extinction than Y-linked suppressors here. By contrast, neutral substitution rates are always equal on the X and Y (as differences in mutational pressure and fixation probabilities balance out), leading to equivalent X-Y contributions to sex chromosome evolution through the fixation of neutral suppressors.

4 Discussion

4.1 Sexual antagonism is likely a key player in sex chromosome evolution

Our analyses indicate that recombination suppressors capturing sexually antagonistic loci generally have a substantially higher probability of invasion and correspondingly lower expected time to substitution than neutral suppressors—except in very small populations or under extreme reproductive variance in the heterogametic sex. This, combined with the fact that sexually antagonistic loci readily maintain balanced polymorphism in the PAR, suggests that sex-specific selection can significantly accelerate the fixation of recombination suppressors beyond neutral expectations. While recombination arrest can, in principle, evolve through the gradual accumulation of neutral or nearly neutral suppressors (Charlesworth and Olito, 2024) along a chromosome (as in e.g., Jay et al., 2022; Lenormand and Roze, 2022, 2024), this is typically slow. Our findings indicate that sexually antagonistic selection can substantially expedite this process; e.g., the presence of even a weakly sexually antagonistic locus ($x_A = -0.5$, $x_a = 0.5$, $\sigma = 0.001$), is sufficient to generate much lower substitution times for Y-linked suppressors under Lenormand and Roze (2022)'s parameters ($\approx 1.5 \times 10^4$ generations instead of 10^5 under neutrality; and this can drop to less than 10^3 generations when sexual antagonism is moderate or strong, see Fig. 3 $\sigma = 0.01, \sigma = 0.1$ curves). Altogether this reinforces the notion that sexual antagonism is likely a key player in the evolution of recombination suppression on sex chromosomes.

Sexually antagonistic selection is particularly potent in driving recombination suppression when

males show heterozygote advantage (for XY systems), which we have shown to be the evolutionary equilibrium for an antagonistic locus on the PAR. Alleles may reach this equilibrium through repeated small-effect mutations, as in our model, though this process may be slow. But male heterozygote advantage could evolve much more rapidly, for instance through large-effect mutations. In fact, mutations that overshoot the male optimum in a single step have the highest invasion fitness and are thus the most likely to invade. Another route for male heterozygote advantage to evolve rapidly is when multiple loci in the PAR contribute to a sexually antagonistic trait, as may occur early-on in sex chromosome evolution when such regions are large (Otto et al., 2011) (we explore this with simulations in Appendix D). Selection in this case quickly sorts out standing variation to generate two predominant haplotypes: one linked to the X-chromosome, with allelic effects summing to half the female optimum, and another linked to the Y-chromosome, with effects overshooting the male optimum. This entails female homozygote advantage (favouring two copies of the X-linked haplotype) and male heterozygote advantage (favouring an X-Y haplotype combination). Therefore, male heterozygote advantage is a plausible and potentially common outcome of sexually antagonistic selection on the PAR, which in turn facilitates the evolution of recombination suppression.

4.2 Recombination arrest may be driven by suppressors on heterogametic or homogametic sex chromosomes

Our analyses also revealed a somewhat unexpected pattern: in XY systems, adaptive recombination suppression is often more likely to be driven by the fixation of X-linked rather than Y-linked modifiers (which had been the focus of previous models, Charlesworth and Charlesworth, 1980; Lenormand and Roze, 2022; Nei, 1969; Olito and Abbott, 2023; Otto, 2014). While a Y-linked suppressor capturing a male-beneficial allele experiences stronger positive selection than an X-linked suppressor capturing a female-beneficial allele (Charlesworth and Charlesworth, 1980), this advantage is insufficient to offset the three-fold difference in X-Y mutational input (owing to the X's larger copy number). This bias towards X-linked suppression is moderate when both sexes show similar fitness distributions, but is amplified in mating systems with high male reproductive variance, as selection is less effective for Y-linked mutations due to the Y's reduced effective population size. By contrast, when recombination suppression evolves neutrally, evolutionary rates on the X and Y are equivalent because X-Y differences in the fixation probabilities of neutral alleles exactly cancel differences in mutational input, irrespective sex-specific drift. In short, adaptive recombination suppression is more likely to be X-linked in the presence of excess male reproductive variance, while neutral suppression is equally

likely to be X- or Y-linked whatever the mating system.

Applying these arguments to ZW systems suggests that when males and females experience similar levels of reproductive variance, recombination suppression should be equally likely to arise from Z- or W-linked factors, with a modest bias towards Z-suppressors under sexually antagonistic selection. However, in polygynous mating systems where males experience elevated reproductive variance, adaptive evolution of the Z is compromised, while the W remains largely unaffected. As a result, in such populations, sexually antagonistic selection should drive recombination suppression through W-linked factors, which experience both stronger positive selection and weaker drift than those on the Z. By contrast, neutral suppression should be unbiased between the Z and W.

By showing that inversions on the heterogametic sex chromosome may be at least as influential as those on the homogametic chromosome in driving recombination suppression, our results provide a potential explanation for the empirical observations of X- and Z-linked inversions along sex chromosomes in a wide range of taxa (e.g., in fish, plants, and flies, Liu et al., 2025; McAllister, 2003; Yue et al., 2023). In particular, Z-linked inversions are thought to have contributed significantly to the evolution of recombination suppression in birds (Zhou et al., 2014). Our results suggest these structural mutations can influence sex-specific adaptation by capturing sexually antagonistic loci. While current data remains limited to draw firm conclusions (Liu et al., 2025), comparing the distribution of sex chromosome inversions across homo- and hetero-gametic chromosomes, especially in species with well-characterised mating systems, may offer a promising approach to delineate the roles of selective and non-selective processes in driving sex chromosome evolution. According to our findings, if such comparisons were to reveal a strong bias towards X-linked inversions in XY systems and W-linked inversions in ZW systems across species with high male reproductive variance, this would implicate sexual antagonism as driving sex chromosome evolution. By contrast, similar occurrences of inversions on X vs Y and Z vs W chromosomes would be more consistent with neutral evolution.

Our results can also provide insight into the relative rates of sex chromosome evolution in XY and ZW systems. In species with stronger male reproductive variance, adaptive recombination suppression should evolve more rapidly in ZW than XY systems (all else being equal), as higher substitution rates for suppressors capturing female-beneficial alleles on the W-chromosome drive faster differentiation. Meanwhile, neutral recombination suppression should proceed equally quickly in XY and ZW systems. Because recombination arrest promotes genetic differentiation between the hetero- and homogametic sex chromosomes—often leading to W and Y degeneration (Bachtrog, 2013)—it is thought to play a key role in sex chromosome turnover (Vicoso, 2019). The “evolutionary trap” model (Pokorna

and Kratochvíl, 2009; Vicoso, 2019) suggests that sex chromosome divergence stabilises a system, for example by generating female-incompatibilities on the Y. By contrast, the "hot potato" model (Blaser et al., 2013, 2014) proposes that degeneration of the heterogametic chromosome favours turnover, as a new sex-determining factor on an autosome can replace a degraded sex chromosome pair. Under both models, our predictions suggest that the stability of XY and ZW systems should differ in polygynous species. Specifically, faster adaptive recombination suppression in ZW systems should accelerate Z-W differentiation, making these systems more stable under the evolutionary trap model but less stable under the hot potato model.

Our study considered explicitly cis-acting recombination modifiers (i.e., those that are in linkage to the SDR and trait loci), and so our results can apply directly to sex chromosome inversions (Kirkpatrick, 2010). However, one relevant factor of inversion biology that we did not consider is that these structural mutations can also induce fitness costs when present in heterozygous form, owing to the production of inviable gametes or zygotes (Berdan et al., 2023, for review). Importantly, if these costs act sex-specifically (which they may well do) then they could have a strong influence on the relative fitnesses of recombination suppressors on different sex chromosomes, and so on the balance of X(Z)-driven vs Y(W)-driven recombination evolution. For example, gamete inviability disproportionately harms females in many species (as sperm production is more weakly correlated with reproductive success than egg production unless males experience strong postcopulatory sexual selection, Janicke et al., 2016; Lehtonen, 2022), and so will penalise the invasion of X- or W-linked suppressors relative to those on the Y or Z. This effect could be sufficient to reverse the X- and W-bias in the basis of suppression evolution. We therefore suggest that incorporating costs of suppression into recombination modifier models may be an important step towards understanding selection on inversions arising on different sex chromosomes. In addition to modifiers acting in cis, recombination can be suppressed by trans-acting factors (Jay et al., 2024) that are unlinked from the SDR and a trait locus (e.g., autosomal modifiers). In such cases, sex-specific selection can have diverse outcomes on recombination rates. In XY systems, selection on trans-acting modifiers can in fact favour the preservation, rather than suppression, of recombination on sex chromosomes. This occurs when males exhibit heterozygote advantage at a trait locus, but females show homozygote advantage for the allele that is at high frequency on the Y (Otto, 2014). However, we find that such a situation does not arise when allelic values diverge through gradual evolution, because the male-beneficial/female-deleterious allele is necessarily the one that increases in frequency on the Y (although it may be possible if a large effect female-beneficial mutation was introduced through male-biased introgression). Our results therefore suggest the evolution of allelic values in the PAR leads to polymorphism that favours recombina-

tion suppression at both cis- and trans- modifiers.

4.3 Conclusion

Sexually antagonistic selection has long been considered a key driver of sex chromosome evolution (Charlesworth and Charlesworth, 1980; Fisher, 1931; Wright et al., 2016), favouring the capture of beneficial alleles by recombination suppressors and accelerating sex chromosome divergence. More recently, this view has been challenged by models suggesting that recombination suppression can arise through other processes (Charlesworth and Olito, 2024; Jay et al., 2022; Lenormand and Roze, 2022; Olito et al., 2024), partly motivated by the difficulty of directly observing sexual antagonism drive recombination evolution. Our results reinforce the notion that sexually antagonistic selection is an important force in recombination evolution, showing that it substantially expedites recombination suppression, especially when allelic divergence generates male heterozygote advantage, which is a likely outcome of evolution on the PAR. Beyond this, our analyses reveal a poorly appreciated pathway for sex chromosome evolution: adaptive recombination suppression may more often be driven by suppressors arising on the homogametic rather than the heterogametic chromosome, a pattern not observed for neutral suppressors. This bias should be especially pronounced in systems with high male reproductive variance, where selection on Y-linked suppressors shows diminished efficacy but selection on the X is largely unaffected. Testing these predictions empirically—especially in taxa where XY and ZW systems show different levels of recombination suppression—will be key to resolving the role of sexual antagonism in shaping sex chromosome evolution.

Acknowledgements

We are grateful to the SNSF for funding (grants PCEFP3181243 and 310030220139) and to Sally Otto for comments on a previous version.

Figures

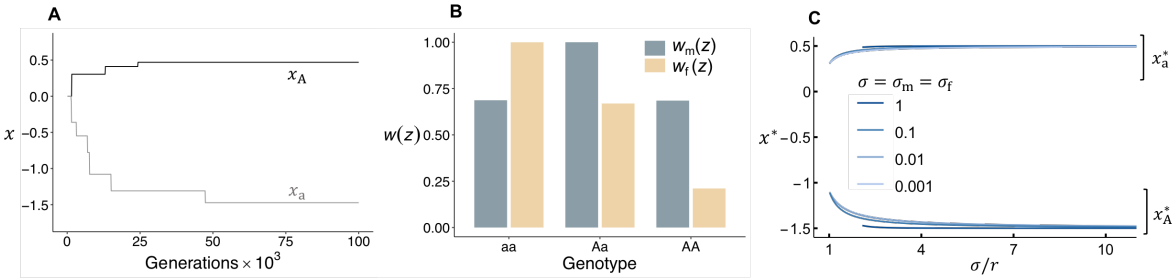

Figure 1: **Evolution of allelic values at a sexually antagonistic locus on the PAR**. Panel **A.** shows the evolution of the allelic values x_a and x_A from individual-based simulations (Appendix A for details). Plot shows the allelic values encoded by the two most frequent alleles at a given generation in a simulation replicate (which correspond to alleles a and A). These values diverge through the accumulation of recurrent mutations, until they converge at $x_a = x_a^* \approx 0.5$ and $x_A = x_A^* \approx -1.5$. Other parameters used in simulation: $N = 10^4, \sigma = \sigma_m = \sigma_f = 0.1, r = 0.005$. Panel **B.** shows the fitness ($w_m(z)$ and $w_f(z)$) of different genotypes (aa, Aa and AA) at generation 10^5 of the simulation in panel **A**, i.e., once allelic values have converged to the evolutionary stable coalition (x_a^*, x_A^*). These show male heterozygote advantage. Panel **C.** shows the evolutionary stable coalition (x_a^*, x_A^*) (see Appendix A for calculation) as a function of the ratio between the strength of sexually antagonistic selection and the recombination rate (σ/r where $\sigma = \sigma_m = \sigma_f$; recall $r < \sigma$ is the condition for disruptive selection in the PAR, hence why some curves do not cover the entire x-axis). Different curves show this for different strengths of σ. Regardless of the strength of sexually antagonistic selection, allelic values at the stable coalition are $x_a^* \approx 0.5$ and $x_A^* \approx -1.5$ unless σ/r is close to 1 (which corresponds to where disruptive selection at the trait locus is weakest). Similar results are found when $\sigma_m \neq \sigma_f$ (see SI Fig. 1).

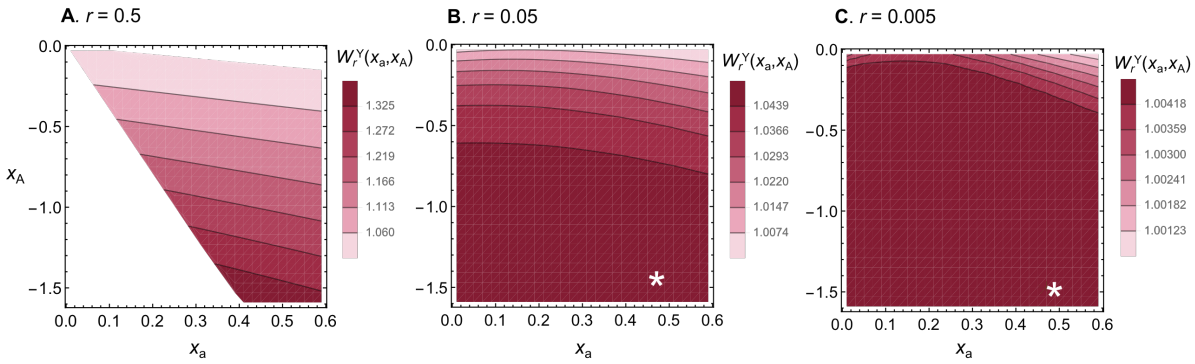

Figure 2: **Invasion fitness of a Y-linked suppressor capturing a trait locus with alleles encoding x_a and x_A.** Plots show the invasion fitness, $W_r^Y(x_a, x_A)$ (main text eq. 3, Appendix B.1 for calculation details), of a Y-linked recombination suppressor capturing allele A at the trait locus as a function of the allelic values x_a and x_A. Different panels show results for different levels of resident recombination between the trait locus and the SDR, r. White stars show the location of the evolutionary stable allelic coalition (x_a^*, x_A^*). Non-coloured space indicates that a suppressor cannot invade (which is because these conditions do not lead to a balanced polymorphism for alleles A and a at the trait locus). Other parameters used $\sigma = \sigma_m = \sigma_f = 0.1$ (see SI Fig. 2 for cases where $\sigma_m \neq \sigma_f$).

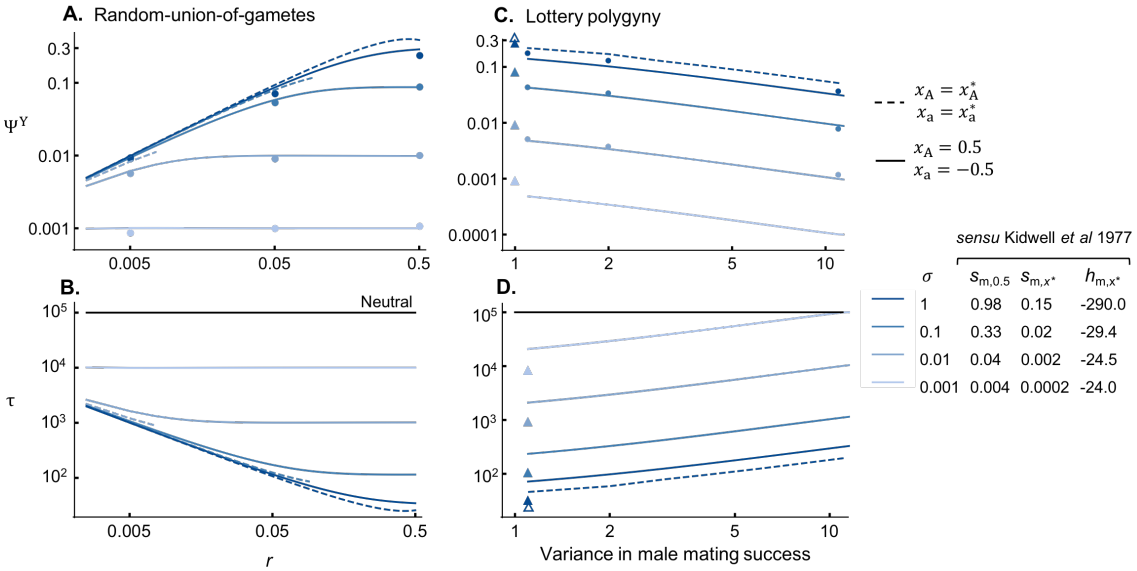

Figure 3: **Invasion probability and waiting times of Y-linked suppressors**. Panel **A.** shows the unconditional invasion probability of a newly arisen Y-linked suppressor, Ψ^Y, under the random-union-of-gametes model (Appendix B.2.1 for calculation) according to the resident recombination rate (r). Dashed lines correspond to invasion probabilities when allelic values have converged to their evolutionary stable coalition (x_a^*, x_A^*) and are therefore shown only for the range of parameters where evolutionary branching occurs. Solid lines correspond to invasion probabilities when allelic values have diverged, but not so much that males show heterozygote advantage: $x_a = 0.5$ and $x_A = -0.5$. Dots show results from individual-based simulations with $x_a = 0.5$ and $x_A = -0.5$ (which correspond to proportion of replicate simulations in which a Y-suppressor fixed, Appendix B.2.2). Different colours correspond to different strengths of selection at the trait locus ($\sigma = \sigma_m = \sigma_f$). Other measures of the strength of selection at the trait locus (following the convention of Kidwell et al., 1977) are also given in the figure table: (1) the male homozygous selection coefficient, $s_m = [w_m(2x_A) - w_m(2x_a)]/w_m(2x_A)$, for allele a (where $s_{m,0.5}$ refers to the case $x_a = 0.5$, $x_A = -0.5$, and s_{m,x^*} to the case $x_a = x_a^*$, $x_A = x_A^*$); (2) the male dominance coefficient for allele a when $x_a = x_a^*$ and $x_A = x_A^*$, $h_{m,x^*} = [w_m(2x_A) - w_m(x_a + x_A)]/(w_m(2x_A) \cdot s_{m,x^*})$ – negative values for h_m indicate male fitness overdominance, and we see large absolute values here because homozygotes show similar fitness when alleles are at their evolutionary stable values; i.e., s_{m,x^*} is very small. Panel **B.** shows the expected waiting time τ for a Y-linked suppressor to substitute into a population of 10^4 males (i.e., $N = 2 \times 10^4$) with mutation rate $\mu = 10^{-5}$ (these are equivalent parameters to those considered by Lenormand and Roze, 2022, their Fig. 2, see Appendix B.2.2 for calculation and further discussion of mutation rates). The same parameter values are used as in panel **A.**. Horizontal black line shows the expected waiting time for a purely neutral Y-linked allele ($1/\mu$). Panels **C.-D.** show the same output as **A.-B.** but for a model of lottery polygyny. In these panels we assume loose linkage $r = 0.5$ between the SDR and trait locus, and vary the degree of variance in male mating success (Appendix B.2.3 for calculation; note that evolutionary branching only occurs when $\sigma > 0.5$ here). Triangles show equivalent Ψ^Y and τ values under the random-union-of-gametes model (empty and filled triangles for $x_a = x_a^*, x_A = x_A^*$ and $x_a = 0.5$, $x_A = -0.5$ cases, respectively).

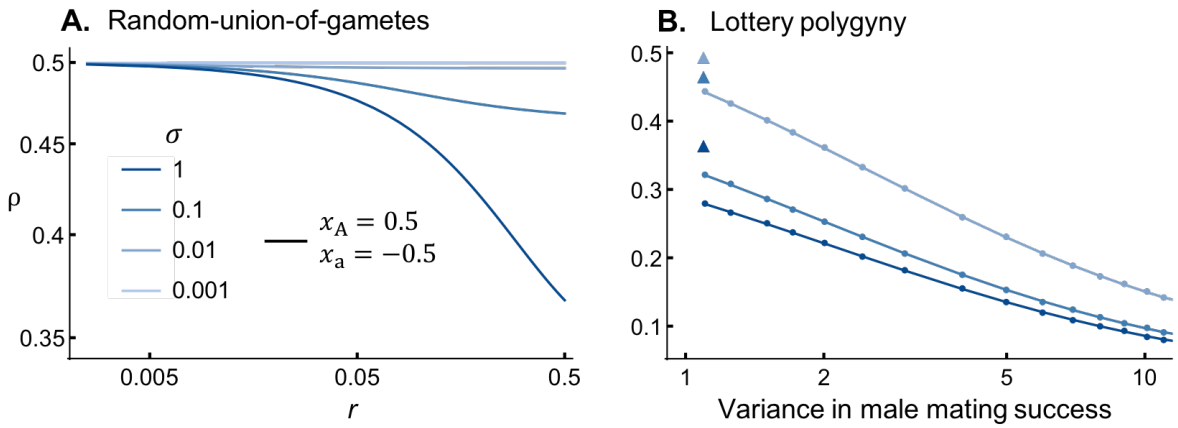

Figure 4: **Likelihood of Y- vs. X-linked suppression**. Plots show the probability that a substitution by a recombination suppressor is X- vs. Y-linked; $\rho = \Psi^{Y}/(\Psi^{Y} + 3\Psi^{X})$ (Appendices B.2.1 and C.2.1 for calculation of Ψ^{X} and Ψ^{Y}, respectively). Panel **A.** shows ρ under the random-union-of-gametes model for different strengths of sexually antagonistic selection ($\sigma = \sigma_m = \sigma_f$, see also Fig. 3 for other measures of the strength of selection) and resident recombination rate r. Lines show results for allelic values $x_a = 0.5, x_A = -0.5$ Panel **B.** shows the same output but for the polygyny model with loose linkage ($r = 0.5$) and different strengths of male mating variance. Here, Ψ^{X} is estimated from individual-based-simulations (coloured dots are individual estimates) while Ψ^{Y} is computed numerically as in Fig. 3 (Appendices B.2.3 and Appendix C.3 for calculation). Triangles show ρ values under the random-union-of-gametes model.

Supplementary Figures

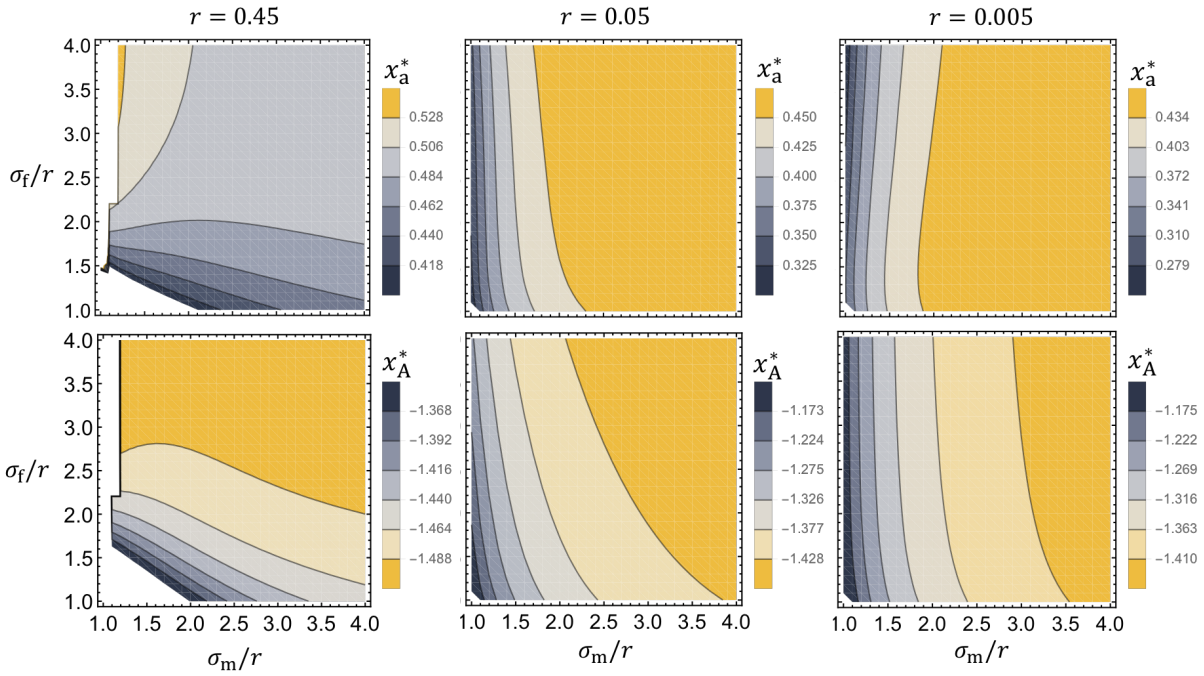

Supplementary Figure 1: **Allelic values at the evolutionary stable coalition** (x_a^*, x_A^*). Top row panels show the allelic value for x_a^* at the stable coalition (x_a^*, x_A^*) (Appendix A for calculation) as a function of the strength of male- and female-selection at the trait locus relative to the recombination rate (σ_m/r and σ_f/r). Bottom rows show equivalent results for the allelic value (x_A^*). Row panels show results for different strengths of recombination between the trait locus and SDR (r). Non-coloured space corresponds to where evolutionary branching at the trait locus does not occur (condition (2) not fulfilled). As seen under strictly symmetric sex-specific selection ($\sigma = \sigma_m = \sigma_f$, Fig. 1C), $x_a^* \approx 0.5$ and $x_A \approx -1.5$ unless sexually antagonistic selection is weak relative to the strength of recombination (σ_m and σ_f small while r big).

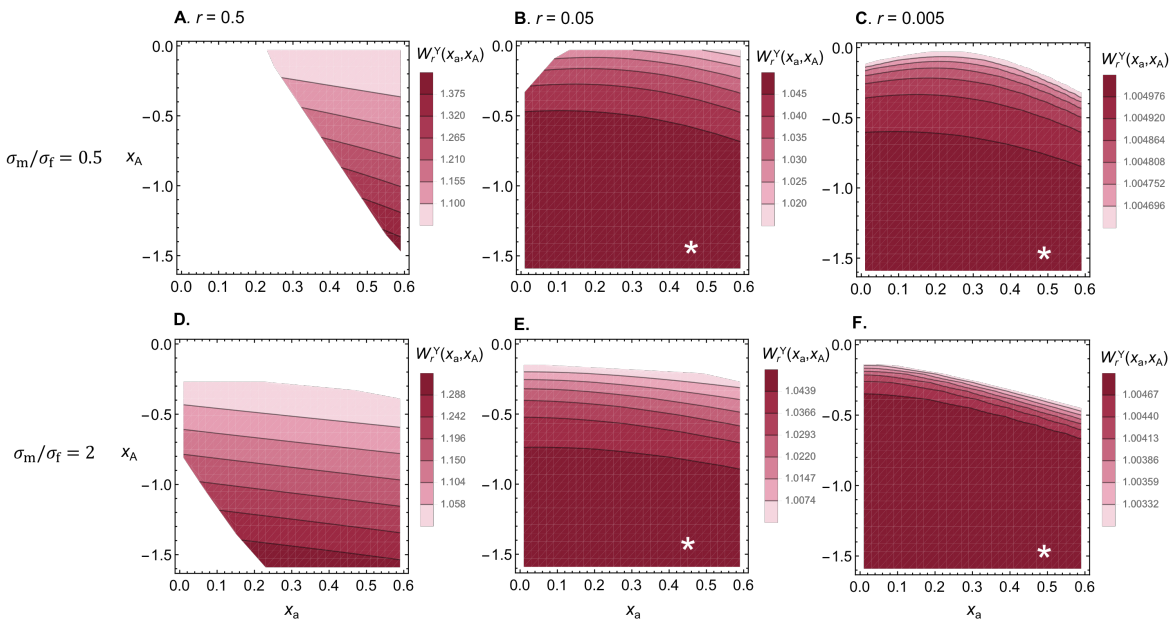

Supplementary Figure 2: **Invasion fitness of a Y-linked suppressor capturing a trait locus with alleles encoding x_a and x_A under sex-biased selection**. Plots show the invasion fitness, $W_r^Y(x_a, x_A)$ (main text eq. 3, Appendix B.1 for calculation details), of a Y-linked recombination suppressor capturing allele A at the trait locus as a function of the allelic values x_a and x_A. Panels **A-C** (top row) show invasion fitness in the presence of female-biased selection at the trait locus ($\sigma_m = 0.075, \sigma_f = 0.15$, so that $\sigma_m/\sigma_f = 0.5$), and panels **D-F** show results for male-biased selection ($\sigma_m = 0.15, \sigma_f = 0.075$, so that $\sigma_m/\sigma_f = 2$). Different row panels show results for different levels of resident recombination between the trait locus and the SDR, r. White star shows the location of the evolutionary stable allelic coalition (x_a^*, x_A^*). Compared to the case of equally strong selection in both sexes (see Fig. 2), the conditions for a Y-linked suppressor to invade are more restrictive under sex-biased selection, which is because such selection is less amenable to the maintenance of a balanced polymorphism at the trait locus (i.e., maintains polymorphism for a narrower range of allelic value combinations; x_a and x_A).

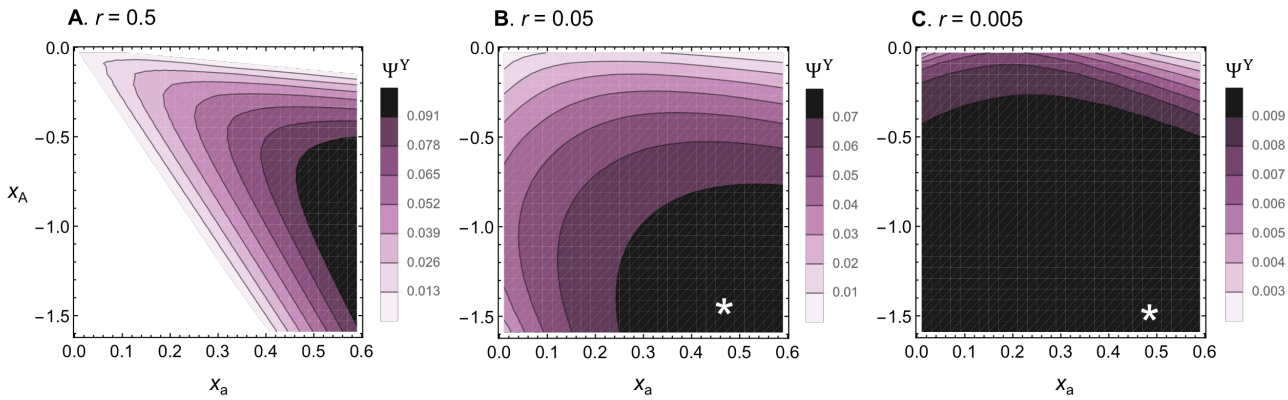

Supplementary Figure 3: **Invasion probability of a Y-linked suppressor capturing a trait locus with alleles encoding x_a and x_A.** Plots show the invasion probability under the random-union-of-gametes model, Ψ^Y (Appendix B.2.1 for calculation details), of a Y-linked recombination suppressor capturing allele A at the trait locus as a function of the allelic values x_a and x_A. Different panels show results for different levels of resident recombination between the trait locus and the SDR, r. White star shows the location of the evolutionary stable allelic coalition (x_a^*, x_A^*). Other parameters used $\sigma = \sigma_m = \sigma_f = 0.1$.

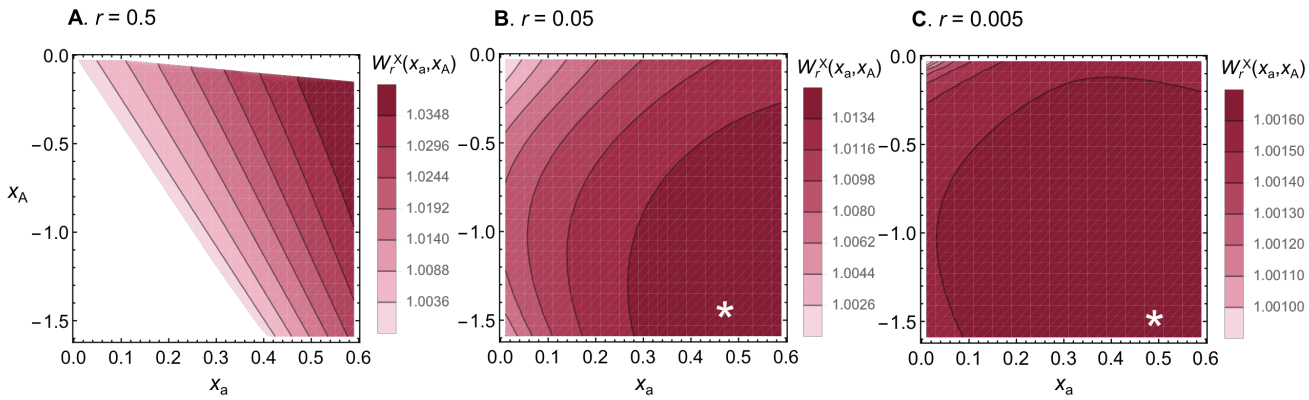

Supplementary Figure 4: **Invasion fitness of an X-linked suppressor capturing a trait locus with alleles encoding x_a and x_A.** Plots show the invasion fitness, $W_r^X(x_a, x_A)$ (main text eq. 3, Appendix C.1 for calculation details), of a Y-linked recombination suppressor capturing allele a at the trait locus as a function of the allelic values x_a and x_A. Different panels show results for different levels of resident recombination between the trait locus and the SDR, r. White stars shows the location of the evolutionary stable allelic coalition (x_a^*, x_A^*). Other parameters used $\sigma = \sigma_m = \sigma_f = 0.1$.

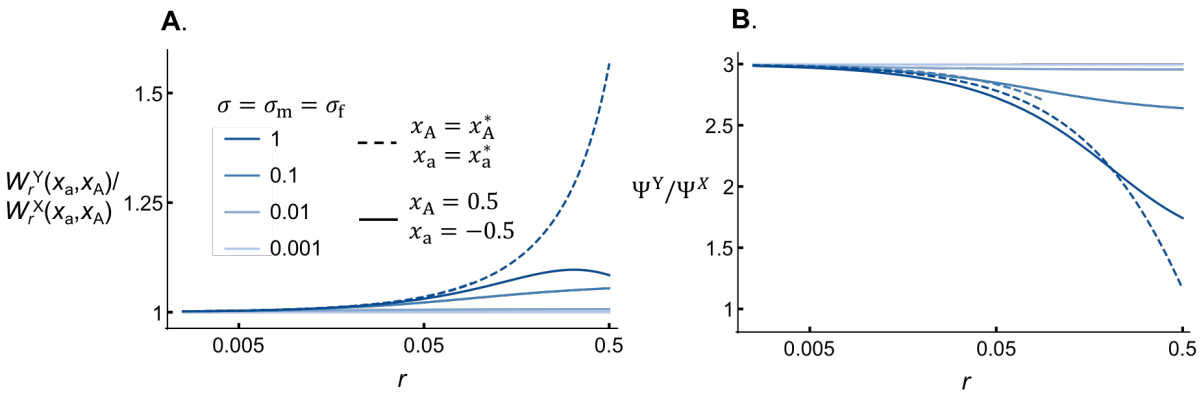

Supplementary Figure 5: **Invasion fitness and invasion probability for Y- vs X-linked suppressors**. Panel **A.** shows the ratio of the invasion fitnesses ($W_r^Y(x_a, x_A)/W_r^X(x_a, x_A)$) of a Y-linked suppressor capturing allele A at the trait locus and an X-linked suppressor capturing allele a for different recombination rates r and strength of sexually antagonistic selection $\sigma = \sigma_m = \sigma_f$. Dashed lines correspond to results for evolutionary stable allelic values (x_a^*, x_A^*) and solid lines for $x_a = 0.5, x_A = -0.5$ (Appendices B.1 and C.1 for calculation of $W_r^Y(x_a, x_A)$ and $W_r^X(x_a, x_A)$). Panel **B.** shows the ratio of the Y- vs X-linked invasion probabilities (Ψ^Y/Ψ^X) under the random-union-of-gametes model for the same parameter combinations and using the same legend as in panel A (Appendices B.2.1 and C.2.1 for calculation of Ψ^Y and Ψ^X).

Appendix to "Sexual antagonism, mating systems, and recombination suppression on sex chromosomes"

Ewan Flintham[1,*] and Charles Mullon[1]

[1]Department of Ecology and Evolution, University of Lausanne, 1015 Lausanne, Switzerland

[*]Correspondence: ewan.flintham@unil.ch

A Evolution of polymorphism on the PAR

A.1 Emergence of polymorphism

In this Appendix we use Flintham et al. (2024) to derive eqs. (1) and (2) of the main text. Under the model given in main text sections 2.1-2.2.1, gradual evolution at a locus under sex-specific selection has been studied with general fitness functions $w_{\mathrm{f}}(z)$ and $w_{\mathrm{m}}(z)$ in Flintham et al. (2024). They showed that selection first drives the population towards a monomorphic equilibrium at $z^* = 2x^*$, around which selection can be stabilising or disruptive according to a condition that depends on the shape of male and female fitness functions and the recombination rate, r.

With Gaussian fitness ($w_{\mathrm{m}}(z) = e^{-\sigma_{\mathrm{m}}(1+z)^2}$ and $w_{\mathrm{f}}(z) = e^{-\sigma_{\mathrm{f}}(-1+z)^2}$), we can find this equilibrium by plugging $w_{\mathrm{m}}(z)$ and $w_{\mathrm{f}}(z)$ into eq. (A-11) in Flintham et al. (2024) and solving for z^*. This readily gives main text eq. (1) (it is also straightforward to see that this equilibrium is always convergence stable, i.e., is an attractor of evolutionary dynamics, by plugging in $w_{\mathrm{m}}(z)$ and $w_{\mathrm{f}}(z)$ into their eq. A-12). Finally, the condition for disruptive selection is found by plugging $w_{\mathrm{m}}(z)$ and $w_{\mathrm{f}}(z)$ into their eq. (E-27), which after some re-arrangements reads as main text condition (2).

If selection is disruptive (i.e. condition (2) of the main text holds), the population will undergo evolutionary branching, leading to the emergence of two alleles (denoted a and A) that are held in a

balanced polymorphism and that undergo further divergence (Geritz et al., 1998). We characterise this second stage of evolution, going beyond Flintham et al. (2024), in the following section.

A.2 Divergence and maintenance polymorphism

A.2.1 Polymorphic dynamics

Under our assumptions, the evolution of allelic values for a and A can be investigated through an invasion analysis that is based on the invasion fitness $W(x_\bullet, x_\mathrm{a}, x_\mathrm{A})$ of a rare mutant encoding an allelic value $x_\bullet$ in a population where resident A and a alleles – encoding x_a and x_A, respectively – are at their equilibrium frequencies (Dercole and Rinaldi, 2008; Geritz et al., 1998; Otto and Day, 2011, chapter 12).

The direction of the evolution of allelic effects a and A is determined by the selection gradient on each genetic value: x_A will evolve according to the sign of $s_\mathrm{A}(x_\mathrm{A}, x_\mathrm{a}) = \partial W(x_\bullet, x_\mathrm{A}, x_\mathrm{a})/\partial x_\bullet|_{x_\bullet = x_\mathrm{A}}$ and x_a to the sign of $s_\mathrm{a}(x_\mathrm{A}, x_\mathrm{a}) = \partial W(x_\bullet, x_\mathrm{A}, x_\mathrm{a})/\partial x_\bullet|_{x_\bullet = x_\mathrm{a}}$. Such evolution may therefore halt at an equilibrium allelic coalition $(x_\mathrm{A}^*, x_\mathrm{a}^*)$ that satisfies

$$s_\mathrm{A}(x_\mathrm{A}^*, x_\mathrm{a}^*) = s_\mathrm{a}(x_\mathrm{A}^*, x_\mathrm{a}^*) = 0. \tag{A-1}$$

This allelic coalition is convergence stable if the real part of the leading eigenvalue of the Jacobian matrix

$$\mathrm{J}(x_\mathrm{a}^*, x_\mathrm{A}^*) = \begin{pmatrix} \dfrac{\partial s_\mathrm{a}(x_\mathrm{A}, x_\mathrm{a})}{\partial x_\mathrm{a}} & \dfrac{\partial s_\mathrm{a}(x_\mathrm{A}, x_\mathrm{a})}{\partial x_\mathrm{A}} \\ \dfrac{\partial s_\mathrm{A}(x_\mathrm{A}, x_\mathrm{a})}{\partial x_\mathrm{a}} & \dfrac{\partial s_\mathrm{A}(x_\mathrm{A}, x_\mathrm{a})}{\partial x_\mathrm{A}} \end{pmatrix}_{\substack{x_\bullet = x_\mathrm{a} = x_\mathrm{a}^* \\ x_\bullet = x_\mathrm{A} = x_\mathrm{A}^*}} \tag{A-2}$$

is negative, and is evolutionarily stable, i.e., there is no further branching once allelic values have converged to x_a^* and x_A^*, if

$$\begin{aligned} \left.\frac{\partial^2 W(x_\bullet, x_\mathrm{A}, x_\mathrm{a})}{\partial x_\mathrm{a}^2}\right|_{x_\bullet = x_\mathrm{a} = x_\mathrm{a}^*} &< 0 \\ \left.\frac{\partial^2 W(x_\bullet, x_\mathrm{A}, x_\mathrm{a})}{\partial x_\mathrm{A}^2}\right|_{x_\bullet = x_\mathrm{A} = x_\mathrm{A}^*} &< 0, \end{aligned} \tag{A-3}$$

in which case the coalition $(x_\mathrm{a}^*, x_\mathrm{A}^*)$ is an endpoint to gradual evolution.

A.2.2 Invasion fitness

We now characterise the invasion fitness $W(x_\bullet, x_\mathrm{A}, x_\mathrm{a})$ of a mutant encoding an allelic value $x_\bullet$ for our model. A mutant allele may initially appear in one of three chromosomal settings: it may arise (i) in an (necessarily X-bearing) egg cell, (ii) in an X-bearing sperm cell, and (iii) in a Y-bearing sperm cell. Its invasion fitness $W(x_\bullet, x_\mathrm{a}, x_\mathrm{A})$ is therefore given by the leading eigenvalue of the mean matrix

$$\mathrm{M}(x_\bullet, x_\mathrm{a}, x_\mathrm{A}) = \begin{pmatrix} W^{\mathrm{f}\to\mathrm{f}}(x_\bullet, x_\mathrm{a}, x_\mathrm{A}) & W^{\mathrm{mX}\to\mathrm{f}}(x_\bullet, x_\mathrm{a}, x_\mathrm{A}) & W^{\mathrm{mY}\to\mathrm{f}}(x_\bullet, x_\mathrm{a}, x_\mathrm{A}) \\ W^{\mathrm{f}\to\mathrm{mX}}(x_\bullet, x_\mathrm{a}, x_\mathrm{A}) & W^{\mathrm{mX}\to\mathrm{mX}}(x_\bullet, x_\mathrm{a}, x_\mathrm{A}) & W^{\mathrm{mY}\to\mathrm{mX}}(x_\bullet, x_\mathrm{a}, x_\mathrm{A}) \\ W^{\mathrm{f}\to\mathrm{mY}}(x_\bullet, x_\mathrm{a}, x_\mathrm{A}) & W^{\mathrm{mX}\to\mathrm{mY}}(x_\bullet, x_\mathrm{a}, x_\mathrm{A}) & W^{\mathrm{mY}\to\mathrm{mY}}(x_\bullet, x_\mathrm{a}, x_\mathrm{A}) \end{pmatrix} \tag{A-4}$$

where $W^{u\to v}(x_\bullet, x_\mathrm{a}, x_\mathrm{A})$ is the expected number of recruited mutant gametes (i.e., that will go on to successfully form a surviving adult individual) of type $v \in \{\mathrm{f}, \mathrm{mX}, \mathrm{mY}\}$ at generation $t+1$ produced by a recruited mutant gamete of type $u \in \{\mathrm{f}, \mathrm{mX}, \mathrm{mY}\}$ at generation t (where superscript f denotes presence in eggs, mX in X-bearing sperm, mY in Y-bearing sperm).

It is straightforward to show that according to the life cycle of the population, the individual components of invasion fitness in eq. (A-4) are

$$\begin{aligned}
W^{\mathrm{f}\to\mathrm{f}}(x_\bullet, x_\mathrm{A}, x_\mathrm{a}) &= \frac{1}{2}\left(\frac{w_\mathrm{f}(x_\bullet + x_\mathrm{a})}{\overline{w}_\mathrm{f}}\left(1-\widehat{p}_\mathrm{m}^\mathrm{X}\right) + \frac{w_\mathrm{f}(x_\bullet + x_\mathrm{A})}{\overline{w}_\mathrm{f}}\widehat{p}_\mathrm{m}^\mathrm{X}\right) \\
W^{\mathrm{mX}\to\mathrm{f}}(x_\bullet, x_\mathrm{A}, x_\mathrm{a}) &= \frac{1}{2}\left(\frac{w_\mathrm{f}(x_\bullet + x_\mathrm{a})}{\overline{w}_\mathrm{f}}\left(1-\widehat{p}_\mathrm{f}\right) + \frac{w_\mathrm{f}(x_\bullet + x_\mathrm{A})}{\overline{w}_\mathrm{f}}\widehat{p}_\mathrm{f}\right) \\
W^{\mathrm{f}\to\mathrm{mX}}(x_\bullet, x_\mathrm{A}, x_\mathrm{a}) &= (1-r)\left(\frac{w_\mathrm{m}(x_\bullet + x_\mathrm{a})}{\overline{w}_\mathrm{m}}\left(1-\widehat{p}_\mathrm{m}^\mathrm{Y}\right) + \frac{w_\mathrm{m}(x_\bullet + x_\mathrm{A})}{\overline{w}_{\mathrm{m},t}}\widehat{p}_\mathrm{m}^\mathrm{Y}\right) \\
W^{\mathrm{mY}\to\mathrm{mX}}(x_\bullet, x_\mathrm{A}, x_\mathrm{a}) &= r\left(\frac{w_\mathrm{m}(x_\bullet + x_\mathrm{a})}{\overline{w}_\mathrm{m}}\left(1-\widehat{p}_\mathrm{f}\right) + \frac{w_\mathrm{f}(x_\bullet + x_\mathrm{A})}{\overline{w}_\mathrm{m}}\widehat{p}_\mathrm{f}\right) \\
W^{\mathrm{f}\to\mathrm{mY}}(x_\bullet, x_\mathrm{A}, x_\mathrm{a}) &= r\left(\frac{w_\mathrm{m}(x_\bullet + x_\mathrm{a})}{\overline{w}_\mathrm{m}}\left(1-\widehat{p}_\mathrm{m}^\mathrm{Y}\right) + \frac{w_\mathrm{m}(x_\bullet + x_\mathrm{A})}{\overline{w}_\mathrm{m}}\widehat{p}_\mathrm{m}^\mathrm{Y}\right) \\
W^{\mathrm{mY}\to\mathrm{mY}}(x_\bullet, x_\mathrm{A}, x_\mathrm{a}) &= (1-r)\left(\frac{w_\mathrm{m}(x_\bullet + x_\mathrm{a})}{\overline{w}_\mathrm{m}}\left(1-\widehat{p}_\mathrm{f}\right) + \frac{w_\mathrm{m}(x_\bullet + x_\mathrm{A})}{\overline{w}_\mathrm{m}}\widehat{p}_\mathrm{f}\right), \\
W^{\mathrm{mY}\to\mathrm{f}}(x_\bullet, x_\mathrm{A}, x_\mathrm{a}) &= W^{\mathrm{mX}\to\mathrm{mY}}(x_\bullet, x_\mathrm{A}, x_\mathrm{a}) = W^{\mathrm{mX}\to\mathrm{mX}}(x_\bullet, x_\mathrm{A}, x_\mathrm{a}) = 0
\end{aligned} \tag{A-5}$$

where $\widehat{p}_\mathrm{f}$, $\widehat{p}_\mathrm{m}^\mathrm{X}$, and $\widehat{p}_\mathrm{m}^\mathrm{Y}$ are the equilibrium frequencies of A in eggs, in X-bearing sperm, and Y-bearing sperm, respectively, and

$$\begin{aligned}
\overline{w}_\mathrm{f} &= \widehat{p}_\mathrm{f}^\mathrm{X}\widehat{p}_\mathrm{f} w_\mathrm{f}(2x_\mathrm{A}) + \left(\widehat{p}_\mathrm{m}^\mathrm{X}(1-p_{\mathrm{f},t}) + (1-\widehat{p}_\mathrm{m}^\mathrm{X})\widehat{p}_\mathrm{f}\right) w_\mathrm{f}(x_\mathrm{A}+x_\mathrm{a}) + (1-\widehat{p}_\mathrm{m}^\mathrm{X})(1-\widehat{p}_\mathrm{f}) w_\mathrm{f}(2x_\mathrm{a}) \\
\overline{w}_\mathrm{m} &= \widehat{p}_\mathrm{m}^\mathrm{Y}\widehat{p}_\mathrm{f} w_\mathrm{m}(2x_\mathrm{A}) + \left(\widehat{p}_\mathrm{m}^\mathrm{Y}(1-\widehat{p}_\mathrm{f}) + (1-\widehat{p}_\mathrm{m}^\mathrm{Y})\widehat{p}_\mathrm{f}\right) w_\mathrm{m}(x_\mathrm{A}+x_\mathrm{a}) + (1-\widehat{p}_\mathrm{m}\mathrm{Y})(1-\widehat{p}_\mathrm{f}) w_\mathrm{m}(2x_\mathrm{a})
\end{aligned} \tag{A-6}$$

are mean female and male fitness when alleles A and a are at their equilibrium frequencies.

To find the equilibrium frequencies $\widehat{p}_{\mathrm{f}}$, $\widehat{p}^{\mathrm{X}}_{\mathrm{m}}$, and $\widehat{p}^{\mathrm{Y}}_{\mathrm{m}}$, we write the frequency of allele A in each chromosome at generation at $t+1$ as

$$\begin{aligned} p^{\mathrm{X}}_{\mathrm{m},t+1} &= M^{\mathrm{X}}(p^{\mathrm{X}}_{\mathrm{m},t}, p^{\mathrm{Y}}_{\mathrm{m},t}, p_{\mathrm{f},t}) \\ p^{\mathrm{Y}}_{\mathrm{m},t+1} &= M^{\mathrm{Y}}(p^{\mathrm{X}}_{\mathrm{m},t}, p^{\mathrm{Y}}_{\mathrm{m},t}, p_{\mathrm{f},t}) \\ p_{\mathrm{f},t+1} &= F(p^{\mathrm{X}}_{\mathrm{m},t}, p^{\mathrm{Y}}_{\mathrm{m},t}, p_{\mathrm{f},t}), \end{aligned} \tag{A-7}$$

where

$$\begin{aligned} M^{\mathrm{X}}(p^{\mathrm{X}}_{\mathrm{m},t}, p^{\mathrm{Y}}_{\mathrm{m},t}, p_{\mathrm{f},t}) &= p^{\mathrm{Y}}_{\mathrm{m},t} p_{\mathrm{f},t} \frac{w_{\mathrm{m}}(2x_{\mathrm{A}})}{\overline{w}_{\mathrm{m},t}} + \left(p^{\mathrm{Y}}_{\mathrm{m},t}(1-p_{\mathrm{f},t})r + (1-p^{\mathrm{Y}}_{\mathrm{m},t})p_{\mathrm{f},t}(1-r)\right)\frac{w_{\mathrm{m}}(x_{\mathrm{A}}+x_{\mathrm{a}})}{\overline{w}_{\mathrm{m},t}} \\ M^{\mathrm{Y}}(p^{\mathrm{X}}_{\mathrm{m},t}, p^{\mathrm{Y}}_{\mathrm{m},t}, p_{\mathrm{f},t}) &= p^{\mathrm{Y}}_{\mathrm{m},t} p_{\mathrm{f},t} \frac{w_{\mathrm{m}}(2x_{\mathrm{A}})}{\overline{w}_{\mathrm{m},t}} + \left(p^{\mathrm{Y}}_{\mathrm{m},t}(1-p_{\mathrm{f},t})(1-r) + (1-p^{\mathrm{Y}}_{\mathrm{m},t})p_{\mathrm{f},t}r\right)\frac{w_{\mathrm{m}}(x_{\mathrm{A}}+x_{\mathrm{a}})}{\overline{w}_{\mathrm{m},t}} \\ F(p^{\mathrm{X}}_{\mathrm{m},t}, p^{\mathrm{Y}}_{\mathrm{m},t}, p_{\mathrm{f},t}) &= p^{\mathrm{X}}_{\mathrm{m},t} p_{\mathrm{f},t} \frac{w_{\mathrm{f}}(2x_{\mathrm{A}})}{\overline{w}_{\mathrm{f},t}} + \frac{1}{2}\left(p^{\mathrm{X}}_{\mathrm{m},t}(1-p_{\mathrm{f},t}) + (1-p^{\mathrm{X}}_{\mathrm{m},t})p_{\mathrm{f},t}\right)\frac{w_{\mathrm{f}}(x_{\mathrm{a}}+x_{\mathrm{A}})}{\overline{w}_{\mathrm{f},t}}, \end{aligned} \tag{A-8}$$

and

$$\begin{aligned} \overline{w}_{\mathrm{f},t} &= p^{\mathrm{X}}_{\mathrm{f},t} p_{\mathrm{f},t} w_{\mathrm{f}}(2x_{\mathrm{A}}) + \left(p^{\mathrm{X}}_{\mathrm{m},t}(1-p_{\mathrm{f},t}) + (1-p^{\mathrm{X}}_{\mathrm{m},t})p_{\mathrm{f},t}\right) w_{\mathrm{f}}(x_{\mathrm{A}}+x_{\mathrm{a}}) + (1-p^{\mathrm{X}}_{\mathrm{m},t})(1-p_{\mathrm{f},t}) w_{\mathrm{f}}(2x_{\mathrm{a}}) \\ \overline{w}_{\mathrm{m},t} &= p^{\mathrm{Y}}_{\mathrm{m},t} p_{\mathrm{f},t} w_{\mathrm{m}}(2x_{\mathrm{A}}) + \left(p^{\mathrm{Y}}_{\mathrm{m},t}(1-p_{\mathrm{f},t}) + (1-p^{\mathrm{Y}}_{\mathrm{m},t})p_{\mathrm{f},t}\right) w_{\mathrm{m}}(x_{\mathrm{A}}+x_{\mathrm{a}}) + (1-p^{\mathrm{Y}}_{\mathrm{m},t})(1-p_{\mathrm{f},t}) w_{\mathrm{m}}(2x_{\mathrm{a}}) \end{aligned} \tag{A-9}$$

(Clark, 1988). Plugging eq. (A-8) into eq. (A-7), we can solve simultaneously for $\widehat{p}_{\mathrm{f}} = p_{\mathrm{f},t+1} = p_{\mathrm{f},t}$, $\widehat{p}^{\mathrm{X}}_{\mathrm{m}} = p^{\mathrm{X}}_{\mathrm{m},t+1} = p^{\mathrm{X}}_{\mathrm{m},t}$ and $\widehat{p}^{\mathrm{Y}}_{\mathrm{m}} = p^{\mathrm{Y}}_{\mathrm{m},t+1} = p^{\mathrm{Y}}_{\mathrm{f},t}$.

A.2.3 Numerical approach

Owing to the complexity of the system eq. (A-7)-(A-9), we could not find analytical expressions for $\widehat{p}_{\mathrm{f}}$, $\widehat{p}^{\mathrm{X}}_{\mathrm{m}}$ and $\widehat{p}^{\mathrm{Y}}_{\mathrm{m}}$. We therefore proceeded to find x^*_{A} and x^*_{a} with a numerical analysis assuming Gaussian fitness functions for $w_{\mathrm{m}}(z)$ and $w_{\mathrm{f}}(z)$. To do so, we iterated the recursions

$$\begin{aligned} x_{\mathrm{a},i+1} &= x_{\mathrm{a},i} + \delta s_{\mathrm{a}}(x_{\mathrm{A},i}, x_{\mathrm{a},i}) \\ x_{\mathrm{A},i+1} &= x_{\mathrm{A},i} + \delta s_{\mathrm{A}}(x_{\mathrm{A},i}, x_{\mathrm{a},i}) \end{aligned} \tag{A-10}$$

with $\delta = 0.1/((\sigma_{\mathrm{m}} + \sigma_{\mathrm{f}})/2)$ (this scaling by σ_{m} and σ_{f} is made for computational expediency, so that changes in allelic values between iterations are not vanishingly small when selection is weak) until

we reached a coalition $(x_{\mathrm{A},i}, x_{\mathrm{a},i})$ that satisfied $|x_{\mathrm{A},i+1} - x_{\mathrm{A},i}| < 10^{-6}$ and $|x_{\mathrm{a},i+1} - x_{\mathrm{a},i}| < 10^{-6}$, which we took to be the equilibrium, i.e. $(x_{\mathrm{A},i}, x_{\mathrm{a},i}) = (x_{\mathrm{A}}^*, x_{\mathrm{a}}^*)$. To calculate $s_{\mathrm{a}}(x_{\mathrm{A},i}, x_{\mathrm{a},i})$ and $s_{\mathrm{A}}(x_{\mathrm{A},i}, x_{\mathrm{a},i})$ at each iteration, we plugged $x_{\mathrm{a},i}$ and $x_{\mathrm{A},i}$ into eqs. (A-8) and eq. (A-9) to find the equilibrium frequencies $\widehat{p}_{\mathrm{f}}, \widehat{p}_{\mathrm{m}}^{\mathrm{X}}$ and $\widehat{p}_{\mathrm{m}}^{\mathrm{Y}}$, then plugged these allelic values and their associated equilibrium frequencies into eq. (A-5), then eq. (A-5) into eq. (A-4), from which we can calculate $s_{\mathrm{a}}(x_{\mathrm{a},i}, x_{\mathrm{A},i})$ and $s_{\mathrm{A}}(x_{\mathrm{a},i}, x_{\mathrm{A},i})$. Finally, we checked that the equilibrium $(x_{\mathrm{a}}^*, x_{\mathrm{A}}^*)$ was convergence and evolutionarily stable by plugging these values into eqs. (A-2)-(A-3), which we found to be satisfied in all cases, indicating that x_{a}^* and x_{A}^* are stable endpoints to gradual evolution. We repeated this procedure with different parameter values ($\sigma_{\mathrm{m}}, \sigma_{\mathrm{f}}$, and r) to produce Fig 1C and SI Fig. 1. In each case, we initialised from a pair of weakly diverged allelic values $(x_{\mathrm{a},1} = 0.01, x_{\mathrm{A},1} = -0.01)$.

A.3 Balanced polymorphism in the PAR

In addition to the evolutionary stable coalition $(x_{\mathrm{a}}^*, x_{\mathrm{A}}^*)$, we also investigate arbitrary allelic values x_{a} and x_{A} that lead to a balanced polymorphism at the trait locus. For such a polymorphism for two alleles encoding x_{a} and x_{A} to exist requires that at least one eigenvalue of the Jacobian matrix

$$\mathrm{J}(x_{\mathrm{a}}, x_{\mathrm{A}}) = \begin{pmatrix} \frac{\partial M^{\mathrm{X}}(p_{\mathrm{m},t}^{\mathrm{X}}, p_{\mathrm{m},t}^{\mathrm{Y}}, p_{\mathrm{f},t})}{\partial p_{\mathrm{m},t}^{\mathrm{X}}} & \frac{\partial M^{\mathrm{X}}(p_{\mathrm{m},t}^{\mathrm{X}}, p_{\mathrm{m},t}^{\mathrm{Y}}, p_{\mathrm{f},t})}{\partial p_{\mathrm{m},t}^{\mathrm{Y}}} & \frac{\partial M^{\mathrm{X}}(p_{\mathrm{m},t}^{\mathrm{X}}, p_{\mathrm{m},t}^{\mathrm{Y}}, p_{\mathrm{f},t})}{\partial p_{\mathrm{f},t}} \\ \frac{\partial M^{\mathrm{Y}}(p_{\mathrm{m},t}^{\mathrm{X}}, p_{\mathrm{m},t}^{\mathrm{Y}}, p_{\mathrm{f},t})}{\partial p_{\mathrm{m},t}^{\mathrm{X}}} & \frac{\partial M^{\mathrm{Y}}(p_{\mathrm{m},t}^{\mathrm{X}}, p_{\mathrm{m},t}^{\mathrm{Y}}, p_{\mathrm{f},t})}{\partial p_{\mathrm{m},t}^{\mathrm{Y}}} & \frac{\partial M^{\mathrm{Y}}(p_{\mathrm{m},t}^{\mathrm{X}}, p_{\mathrm{m},t}^{\mathrm{Y}}, p_{\mathrm{f},t})}{\partial p_{\mathrm{f},t}} \\ \frac{\partial F(p_{\mathrm{m},t}^{\mathrm{X}}, p_{\mathrm{m},t}^{\mathrm{Y}}, p_{\mathrm{f},t})}{\partial p_{\mathrm{m},t}^{\mathrm{X}}} & \frac{\partial F(p_{\mathrm{m},t}^{\mathrm{X}}, p_{\mathrm{m},t}^{\mathrm{Y}}, p_{\mathrm{f},t})}{\partial p_{\mathrm{m},t}^{\mathrm{Y}}} & \frac{\partial F(p_{\mathrm{m},t}^{\mathrm{X}}, p_{\mathrm{m},t}^{\mathrm{Y}}, p_{\mathrm{f},t})}{\partial p_{\mathrm{f},t}} \end{pmatrix}_{p_{\mathrm{m},t}^{\mathrm{X}} = p_{\mathrm{m},t}^{\mathrm{Y}} = p_{\mathrm{f},t} = p} \tag{A-11}$$

is greater than one for both $p = 0$ and $p = 1$ (which indicates reciprocal invasion of alleles A and a), where the functions $M^{\mathrm{X}}(p_{\mathrm{m},t}^{\mathrm{Y}}, p_{\mathrm{m},t}^{\mathrm{Y}}, p_{\mathrm{f},t}), M^{\mathrm{Y}}(p_{\mathrm{m},t}^{\mathrm{Y}}, p_{\mathrm{m},t}^{\mathrm{Y}}, p_{\mathrm{f},t})$ and $F(p_{\mathrm{m},t}^{\mathrm{Y}}, p_{\mathrm{m},t}^{\mathrm{Y}}, p_{\mathrm{f},t})$ are detailed in eq. (A-8).

B Evolution of a Y-linked suppressor

B.1 Invasion fitness

Here, we characterise the invasion fitness of a Y-linked recombination suppressor appearing as a single copy in a recruited Y-bearing sperm (i.e., that successfully goes on to form an adult male). This

mutant appears arises in a population that recombines at a resident rate r and that is at a polymorphic equilibrium at the trait locus – i.e., where alleles A and a are at their equilibrium frequencies given by $\widehat{p}_{\mathrm{f}}$, $\widehat{p}^{\mathrm{X}}_{\mathrm{m}}$ and $\widehat{p}^{\mathrm{Y}}_{\mathrm{m}}$. Such a mutant arises in a Y-bearing sperm carrying allele A with probability $\widehat{p}^{\mathrm{Y}}_{\mathrm{m}}$ and one carrying allele a with probability $1-\widehat{p}^{\mathrm{Y}}_{\mathrm{m}}$. Let us denote with $W^{\mathrm{Y}}_{r,\mathrm{A}}(x_{\mathrm{a}},x_{\mathrm{A}})$ and $W^{\mathrm{Y}}_{r,\mathrm{a}}(x_{\mathrm{a}},x_{\mathrm{A}})$ the invasion fitness for each of these two cases respectively. Since we assume the suppressor fully arrests recombination with the trait locus, these are given by

$$W^{\mathrm{Y}}_{r,\mathrm{A}}(x_{\mathrm{a}},x_{\mathrm{A}}) = \frac{w_{\mathrm{m}}(x_{\mathrm{a}}+x_{\mathrm{A}})}{\overline{w}_{\mathrm{m}}}(1-\widehat{p}_{\mathrm{f}}) + \frac{w_{\mathrm{m}}(2x_{\mathrm{A}})}{\overline{w}_{\mathrm{m}}}\widehat{p}_{\mathrm{f}} \tag{B-1a}$$

$$W^{\mathrm{Y}}_{r,\mathrm{a}}(x_{\mathrm{a}},x_{\mathrm{A}}) = \frac{w_{\mathrm{m}}(2x_{\mathrm{a}})}{\overline{w}_{\mathrm{m}}}(1-\widehat{p}_{\mathrm{f}}) + \frac{w_{\mathrm{m}}(x_{\mathrm{a}}+x_{\mathrm{A}})}{\overline{w}_{\mathrm{m}}}\widehat{p}_{\mathrm{f}}, \tag{B-1b}$$

where recall $\overline{w}_{\mathrm{m}} = (1-\widehat{p}^{\mathrm{Y}}_{\mathrm{m}})(1-\widehat{p}_{\mathrm{f}})w_{\mathrm{m}}(2x_{\mathrm{a}}) + \widehat{p}^{\mathrm{Y}}_{\mathrm{m}}\widehat{p}_{\mathrm{f}}w_{\mathrm{m}}(2x_{\mathrm{A}}) + (\widehat{p}^{\mathrm{Y}}_{\mathrm{m}}+\widehat{p}_{\mathrm{f}}-2\widehat{p}^{\mathrm{Y}}_{\mathrm{m}}\widehat{p}_{\mathrm{f}})w_{\mathrm{m}}(x_{\mathrm{a}}+x_{\mathrm{A}})$ is mean male fitness with allele frequencies (eq. B-1a is main text eq. 3, see also Olito and Abbott, 2023 eq. 15 and Appendix C for an alternative derivation).

For a suppressor to invade given it arises with allele A or with allele a, we must have $W^{\mathrm{Y}}_{r,\mathrm{A}}(x_{\mathrm{a}},x_{\mathrm{A}}) > 1$ and $W^{\mathrm{Y}}_{r,\mathrm{a}}(x_{\mathrm{a}},x_{\mathrm{A}}) > 1$, respectively. We first argue that $W^{\mathrm{Y}}_{r,\mathrm{a}}(x_{\mathrm{a}},x_{\mathrm{A}}) > 1$ never holds. We do so by noting first that once alleles A and a have diverged (i.e., $x_{\mathrm{A}} < x_{\mathrm{a}}$), additive gene action entails that male heterozygotes show higher fitness than those homozygous for allele a (i.e., $w_{\mathrm{m}}(x_{\mathrm{a}}+x_{\mathrm{A}}) > w_{\mathrm{m}}(2x_{\mathrm{a}})$). Allele A can then either : (I) be strictly male-beneficial: $w_{\mathrm{m}}(2x_{\mathrm{a}}) < w_{\mathrm{m}}(x_{\mathrm{a}}+x_{\mathrm{A}}) < w_{\mathrm{m}}(2x_{\mathrm{A}})$, or (II) lead males to show heterozygote advantage: $w_{\mathrm{m}}(x_{\mathrm{a}}+x_{\mathrm{A}}) > w_{\mathrm{m}}(2x_{\mathrm{a}})$ and $w_{\mathrm{m}}(x_{\mathrm{a}}+x_{\mathrm{A}}) > w_{\mathrm{m}}(2x_{\mathrm{A}})$. In scenario (I), with some rearrangements of eq. (B-1b), it is straightforward to show that $W^{\mathrm{Y}}_{r,\mathrm{a}}(x_{\mathrm{a}},x_{\mathrm{A}}) < 1$ for all $\widehat{p}_{\mathrm{f}}$, $\widehat{p}^{\mathrm{Y}}_{\mathrm{m}}$ and all x_{a} and x_{A} (with $x_{\mathrm{A}} < x_{\mathrm{a}}$), so that a suppressor capturing allele a cannot invade. In scenario (II), rearranging eq. (B-1b) shows a suppressor can invade if the following condition holds

$$\widehat{p}_{\mathrm{f}} > \frac{w_{\mathrm{m}}(x_{\mathrm{a}}+x_{\mathrm{A}}) - w_{\mathrm{m}}(2x_{\mathrm{a}})}{2w_{\mathrm{m}}(x_{\mathrm{a}}+x_{\mathrm{A}}) - w_{\mathrm{m}}(2x_{\mathrm{a}}) - w_{\mathrm{m}}(2x_{\mathrm{A}})}. \tag{B-2}$$

This requires the equilibrium frequency of allele A be large relative to the fitness advantage of male heterozygotes. We evaluated this condition for a large range of allelic values x_{a} and x_{A} satisfying $w_{\mathrm{m}}(x_{\mathrm{a}}+x_{\mathrm{A}}) > w_{\mathrm{m}}(2x_{\mathrm{A}})$ and that would result in a balanced polymorphism at the trait-locus (Appendix A.3; including the equilibrium $(x^*_{\mathrm{a}}, x^*_{\mathrm{A}})$), strengths of selection (σ_{m} and σ_{f}), and recombination rates r numerically (using eqs. A-7-A-8 to find the equilibrium frequencies for alleles A and a, and inserting these values into eqs. 4b and B-2). Among 1000 parameter sets tested in $\sigma_{\mathrm{m}} \in [0.0001, 1], \sigma_{\mathrm{f}} \in [0.0001, 1], r \in [0.0025, 0.5], x_{\mathrm{a}} \in [0.01, 0.5], x_{\mathrm{A}} \in [-0.01, -1.6]$ we found none such that condition (B-2) is fulfilled.

By contrast, using the same arguments, we find that $W^{\mathrm{Y}}_{r,\mathrm{A}}(x_{\mathrm{a}}, x_{\mathrm{A}}) > 1$ always holds: When A is male-beneficial (scenario I above), it is straightforward to show that $W^{\mathrm{Y}}_{r,\mathrm{A}}(x_{\mathrm{a}}, x_{\mathrm{A}}) > 1$ is satisfied for all $\widehat{p}_{\mathrm{f}}, \widehat{p}^{\mathrm{Y}}_{\mathrm{m}}, x_{\mathrm{a}}$, and x_{A}; main text condition (4a). Whereas, if males show heterozygote advantage (scenario II above), then $W^{\mathrm{Y}}_{r,\mathrm{A}}(x_{\mathrm{a}}, x_{\mathrm{A}}) > 1$ when

$$\widehat{p}_{\mathrm{f}} < \frac{w_{\mathrm{m}}(x_{\mathrm{a}} + x_{\mathrm{A}}) - w_{\mathrm{m}}(2x_{\mathrm{a}})}{2w_{\mathrm{m}}(x_{\mathrm{a}} + x_{\mathrm{A}}) - w_{\mathrm{m}}(2x_{\mathrm{a}}) - w_{\mathrm{m}}(2x_{\mathrm{A}})} \tag{B-3}$$

(given as main text condition 4b – eq. B-3 is the mirror image of eq. B-2). Performing the same numerical analysis as for condition eq. (B-2), we found that eq. (B-3) was fulfilled for all 1000 parameter sets we tested in $\sigma_{\mathrm{m}} \in [0.0001, 1], \sigma_{\mathrm{f}} \in [0.0001, 1], r \in [0.0025, 0.5], x_{\mathrm{a}} \in [0.01, 0.5], x_{\mathrm{A}} \in [-0.01, -1.6]$.

Having established that the capture of allele A is both a necessary and sufficient condition for invasion of a Y-linked suppressor, to simplify notation we drop the dependency of W^{Y}_{r} on allele type and use it to refer to the invasion fitness of a recombination suppressor conditional on it capturing allele A, i.e., $W^{\mathrm{Y}}_{r}(x_{\mathrm{a}}, x_{\mathrm{A}}) = W^{\mathrm{Y}}_{r,\mathrm{A}}(x_{\mathrm{a}}, x_{\mathrm{A}})$ (this notation is also used in the main text).

We next investigated how the strength of positive selection on a suppressor capturing allele A, measured by the magnitude of invasion fitness (i.e., how much greater than unity $W^{\mathrm{Y}}_{r}(x_{\mathrm{a}}, x_{\mathrm{A}})$ is), depends on allelic values (x_{a} and x_{A}), the strength of Gaussian sex-specific selection (σ_{m} and σ_{f}), and the recombination rate (r). As before, we used eqs. (A-7)-(A-8) to solve for $\widehat{p}_{\mathrm{f}}, \widehat{p}^{\mathrm{X}}_{\mathrm{m}}$ and $\widehat{p}^{\mathrm{Y}}_{\mathrm{m}}$ for a wide range of parameter sets that precipitate a balanced polymorphism at the trait locus (Appendix A.3), and plugged these frequencies and their associated parameters into eq. (B-1a) in order to produce Fig. 2. These results are interpreted in main text section 3.2.

B.2 Probability of invasion and substitution times under random mating

B.2.1 Probability of invasion

As a next step in our analysis, we calculate the probability Ψ^{Y} that a Y-linked suppressor that has arisen as a single copy successfully invades, i.e. evades stochastic loss. From Appendix B.1 and standard branching process theory, we know that a Y-linked suppressor is only under positive selection when it captures allele A; otherwise the suppressor experiences negative selection and so goes extinct with probability 1 when found as a single copy. The (unconditional) invasion probability of a suppressor can therefore be expressed as $\Psi^{\mathrm{Y}} = \widehat{p}^{\mathrm{Y}}_{\mathrm{m}}\Psi^{\mathrm{Y}}_{\mathrm{A}}$. Here, $\widehat{p}^{\mathrm{Y}}_{\mathrm{m}}$ is the frequency of allele A in Y-bearing sperm, and so gives the probability a Y-linked suppressor captures allele A, and $\Psi^{\mathrm{Y}}_{\mathrm{A}}$ is the (conditional)

probability a suppressor invades given it captured allele A.

This conditional invasion probability can be calculated using a branching process argument (Haldane, 1927; Otto and Whitlock, 2001) by solving

$$1 - \Psi_{\mathrm{A}}^{\mathrm{Y}} = \sum_{j=0}^{\infty} \Pr(X = j)(1 - \Psi_{\mathrm{A}}^{\mathrm{Y}})^{j}, \tag{B-4}$$

where X is a random variable denoting the number of copies produced by a rare suppressor that has captured allele A over one generation (such that $\Pr(X = j)$ for $j \in \{0, 1, \ldots\}$ gives the probability mass function of suppressor fitness). Equivalently X is a random variable for the number of surviving male offspring produced by a male carrying the suppressor mutation.

Under the lifecycle given in section 2.1 (i.e. the random-union-of-gametes), X follows a Poisson distribution with mean given by $W_r^{\mathrm{Y}}(x_{\mathrm{a}}, x_{\mathrm{A}})$ (shown in eq. B-1a), i.e. $X \sim \mathrm{Pois}\left(W_r^{\mathrm{Y}}(x_{\mathrm{a}}, x_{\mathrm{A}})\right)$ so that

$$\Pr(X = j) = \frac{W_r^{\mathrm{Y}}(x_{\mathrm{a}}, x_{\mathrm{A}})^{j} \exp\left(-W_r^{\mathrm{Y}}(x_{\mathrm{a}}, x_{\mathrm{A}})\right)}{j!} \tag{B-5}$$

(we consider alternative mating system, leading to a different form for $\Pr(X = j)$ in Appendix B.2.3). Substituting eq. (B-5) into eq. (B-4), we obtain

$$1 - \Psi_{\mathrm{A}}^{\mathrm{Y}} = \exp\left(-W_r^{\mathrm{Y}}(x_{\mathrm{a}}, x_{\mathrm{A}})\Psi_{\mathrm{A}}^{\mathrm{Y}}\right), \tag{B-6}$$

which cannot be solved in general.

To generate our main text results, we take a numerical approach and calculate Ψ^{Y} across a wide range of allelic values x_{a} and x_{A} (including the equilibrium values x_{a}^{*} and x_{A}^{*}), strengths of Gaussian sex-specific selection σ_{m} and σ_{f}, and resident recombination rate r. This involved (1) calculating the equilibrium allele frequencies $\widehat{p}_{\mathrm{f}}$ and $\widehat{p}_{\mathrm{m}}^{\mathrm{Y}}$ and invasion fitness $W_r^{\mathrm{Y}}(x_{\mathrm{a}}, x_{\mathrm{A}})$ (numerically as per Appendices A.2.2 and B.1) for a given allelic coalition $(x_{\mathrm{a}}, x_{\mathrm{A}})$ and parameter set ($\sigma_{\mathrm{m}}, \sigma_{\mathrm{f}}$ and r); (2) plugging $W_r^{\mathrm{Y}}(x_{\mathrm{a}}, x_{\mathrm{A}})$ into eq. (B-6) and solving numerically for the conditional invasion probability $\Psi_{\mathrm{A}}^{\mathrm{Y}}$; (3) multiplying $\Psi_{\mathrm{A}}^{\mathrm{Y}}$ by $\widehat{p}_{\mathrm{m}}$ to give the unconditional probability Ψ^{Y}. Our results for Ψ^{Y} are shown in Fig. 3A and SI Fig. 3 and interpreted in main text section 3.3.

Our analysis here can be connected to that of Olito and Abbott (2023), who also calculate the unconditional invasion probability $\Psi_{\mathrm{A}}^{\mathrm{Y}}$ for a Y-linked recombination suppressor that captures a sexually antagonistic locus with fixed additive fitness effects (specifically where $w_{\mathrm{f}}(2x_{\mathrm{a}}) = 1$, $w_{\mathrm{f}}(x_{\mathrm{a}} + x_{\mathrm{A}}) = 1 - s_{\mathrm{f}}/2$,

$w_f(2x_A) = 1 - s_f$, $w_m(2x_a) = 1 - s_m$, $w_m(x_a + x_A) = 1 - s_m/2$, $w_m(2x_A) = 1$ and $0 \le s_m < 1$ and $0 \le s_m < 1$). Olito and Abbott (2023) use eq. (B-1a) to calculate $W_r^Y(x_a, x_A)$ for a Y-suppressor capturing the strictly male-beneficial allele A and then use the approximation $\Psi_A^Y = 2s_r$ where $s_r = W_r^Y(x_a, x_A) - 1$. This works well when selection on a modifier is weak (s_r is small; e.g., under the branching process, writing $W_r^Y(x_a, x_A) = 1 + s_r$, where $s_r \ll 1$, gives $\Psi_A^Y = 2(W_r^Y(x_a, x_A) - 1) + \mathcal{O}(s_r^2))$, but strongly overestimates invasion probabilities when selection is strong (Otto and Whitlock, 2001), and so is more limited for studying recombination suppression when polymorphism evolves at PAR loci far from the SDR-boundary (r and σ large), as we do here.

B.2.2 Fixation and substitution

Our results thus far have concerned the dynamics of a suppressor as it invades into a population from a single copy. However, the tempo of recombination evolution depends not just on how frequently such suppressors invade, but also on whether they go on to fix in the population, the conditions for which may diverge from those for invasion. In particular, a large effect mutation such as a full recombination suppressor (i.e., that completely silences recombination) that invades into a population may be prevented from fixing if it experiences negative frequency-dependent selection – in which case the suppressor is held at an intermediate frequency as a balanced polymorphism.

To establish whether a Y-linked suppressor that has successfully invaded into a population will go on to fix or not, we ran individual-based simulations of a Wright-Fisher process using SLiM 4,0 (Haller and Messer, 2023) that track the frequency of a suppressor through time. Following the lifecycle in section 2.1, we simulate a diploid population of $N = 10^4$ adults with non-overlapping generations, where each individual carries a single chromosome with three loci: one XY sex-determining locus, one modifier locus that is in full linkage with the sex-determining locus, and one trait locus recombining with the sex-determining locus at rate r). At each generation, 5000 male and 5000 female individuals are created through multinomial sampling of adult males and females from the previous generation, with a sample weighting given by their fecundity ($w_m(z)$ and $w_f(z)$, which as we assume are Gaussian, where z is given by the sum of the values encoded by the alleles they carry at the trait locus). We assume the trait locus is polymorphic for alleles A and a and we initialise simulations with alleles at their equilibrium frequencies in all gene pools ($\hat{p}_m^X, \hat{p}_m^Y$ and $\hat{p}_f$; to ensure one allele is not lost by chance during the simulation, we allow mutations between the two alleles at a per-locus rate 5×10^{-5}).

At the beginning of each simulation, we introduce a suppressor mutant into the population, doing so in one of two different ways: (1) In one set of simulations, we introduce a single copy into the population (i.e., with initial frequency $1/(N/2)$), which is placed in the Y-chromosome of a randomly sampled male. This setup therefore follows our previous analyses in considering the fate of a novel suppressor (providing a comparison for our invasion results). (2) In a second set of simulations, we introduced the mutant into $qN/2$ (rounded to the nearest integer) randomly sampled A-bearing adult male Y-chromosomes, where $q = 1/(\Psi^{\mathrm{Y}}_{\mathrm{A}} N/2)$ is the frequency at which a mutant suppressor that originally arose a single copy in a chromosome containing A can be considered to have invaded (i.e., to have avoided stochastic loss when rare in a large population, Charlesworth, 2020; Maynard Smith, 1976). In other words, here we are following the trajectory of a suppressor, conditional on it successfully establishing in the population. In both cases, we ran simulations until the suppressor either fixed or went extinct in the population, doing so for the same range of parameter/allelic value combinations considered in section B.2.1, with 10^4 replicates for each parameter set.

For all parameter sets considered we found: (1) In simulations where a suppressor was introduced as a single copy, the proportion of replicates in which the mutant fixed closely matched the unconditional invasion probability, Ψ^{Y}, calculated in Appendix B.2.1 (some example values are plotted in Fig 3A, and the frequency trajectories of some example simulations are shown in Appendix Fig. 1A). (2) in simulations where the mutant was introduced at frequency q, we found that it always quickly swept to fixation. Together, these observations strongly suggest that successful invasion by a Y-suppressor is sufficient for its eventual fixation (i.e., selection on recombination suppressors is not frequency dependent even when selection is strong; this is consistent with the results of Olito and Abbott, 2023 Appendix C, and extends the weak selection results of Otto, 2014 who found that the invasion conditions for small effect recombination promoters and suppressors are mutually exclusive). Consequently, we consider that Ψ^{Y} captures both the probability of invasion and fixation for a Y-linked suppressor.

With this in mind, we can use our invasion results to calculate the expected waiting time for such a suppressor to substitute (to appear in a population and then go on to fix). To do this, we assume suppressor mutants arise in a population at a low constant rate $\lambda_\mu = (N/2)\mu \ll 1$ per generation (where μ is the probability a novel suppressor mutant appears in a given Y-bearing gamete), such that substitution is a Poisson process with rate $\lambda_{\mathrm{sub}} = \lambda_\mu \Psi^{\mathrm{Y}}$. From this it follows that the random variable T giving the waiting time (number of generations) for the substitution to occur is exponentially distributed

$T \sim \text{Exponential}(\lambda_{\text{sub}})$, and therefore with mean

$$\tau = \mathrm{E}[T] = 1/\lambda_{\text{sub}}. \tag{B-7}$$

To generate our main text Fig. 3B we plugged the values for Ψ^{Y} calculated numerically into eq. (B-7), which we compared against the neutral substitution time: $1/\mu$. In our figures we used a large population size 10^4 and a gametic mutation rate of 10^{-5} (as in Lenormand and Roze, 2022), although equivalent results are produced with weaker mutation rates. Recent estimates (Berdan et al., 2021, box 1) place genome-wide gametic mutation rates for recombination suppressors such as inversions at $\approx 10^{-3}$ (and chromosomal fusions at $\approx 10^{-4}$), thus our parameters are consistent with 1% of these mutations occurring on the Y-chromosome and capturing the SDR.

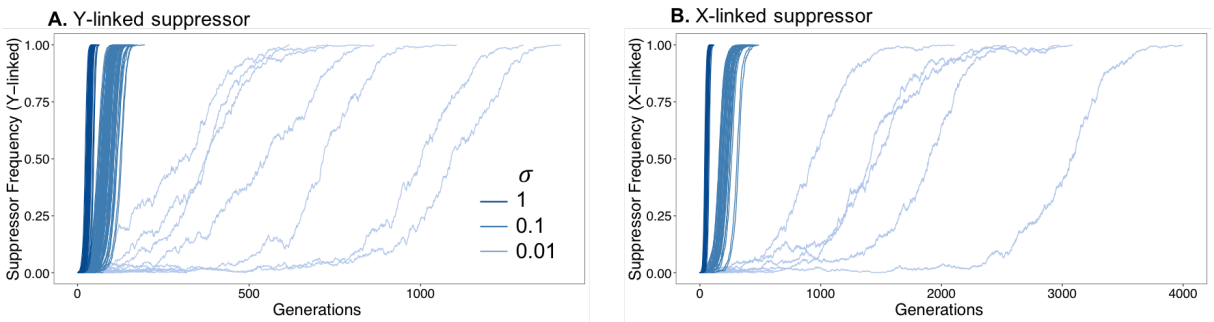

Appendix Figure 1: **Frequency of Y- and X-linked suppressors through time from example simulations**. Plots show suppressor frequency through time in example simulations where a suppressor was introduced as a single copy (Appendix B.2.2 and C.2.2 for details). Panels **A.** and **B.** respectively show frequency trajectories for simulations where a Y-linked and X-linked suppressor was introduced and different colour curves show replicates with different strengths of sexually antagonistic selection ($\sigma = \sigma_{\text{f}} = \sigma_{\text{m}}$, other parameters: $x_{\text{a}} = 0.5, x_{\text{A}} = -0.5, r = 0.5$). A sample of 1000 replicate simulations is shown for each treatment, with two mutually exclusive types of trajectories being observed for both Y- and X-linked suppressors: (1) suppressor frequency remains low after its introduction, and the mutant ends up being lost quickly, (2) suppressors rapidly sweep to fixation at a rate sensitive to σ (notice curve show the characteristic sigmoid-shape consistent with a sweep occurring). This pattern supports the notion that suppressors that successfully invade into a population systematically go on to fix.

B.2.3 Probability of invasion under polygyny

Here, we consider the invasion probability Ψ^{Y} under a model of lottery polygyny (Nunney, 1993). To do so, we can still use eq. (B-4) but X should now be non-Poisson. We determine the probability mass function $\Pr(X = j)$ under a lifecycle similar to the one analysed by Lee et al. (2008). This life-cycle is as follows : (1) $N/2$ adult males and $N/2$ adult females enter the mating pool (where N is large). Fe-

males mate singly but males can mate multiply. For each female, a male is sampled with replacement to mate and sire all her offspring. The probability of each male $i \in \{1, \ldots, N/2\}$ of being sampled is weighted by his competitiveness which we denote as c_i (e.g., c_i represents a male's biological condition, or level of expression of a sexually selected ornament relative to other males in the population). (2) After mating, females produce a large number of juveniles (in this model, male mating success and female fecundity are independent of genotype). (3) Adults die and juveniles undergo sex-specific density-dependent competition for access to $N/2$ male and $N/2$ female adult positions in the mating pool of the next generation. This competition is mediated by the evolving trait z; i.e. the relative probability of surviving to the mating pool of a juvenile male expressing trait z is $w_{\mathrm{m}}(z)$, while that of a female is $w_{\mathrm{f}}(z)$. This ensures that the expected number of surviving offspring of males and females expressing a trait value z is identical to that in the random-union-of-gametes model (section 2.1) and therefore leads to equivalent sexually antagonistic selection in both models, allowing us to focus on the effects of mating system on reproductive variance.

For this model of polygyny, we can obtain the probability mass function $\Pr(X = j)$ for the number X of males produced by a mutant male using conditional probabilities :

$$\Pr(X = j) = \sum_{m=0}^{N/2} \sum_{\boldsymbol{f} \in \mathscr{F}} \Pr(X = j | \boldsymbol{F} = \boldsymbol{f}) \Pr(\boldsymbol{F} = \boldsymbol{f} | M = m) \Pr(M = m), \tag{B-8}$$

where M is the random variable for the number of females mated by a mutant male, and $\boldsymbol{F} = (F_{\mathrm{aa}}, F_{\mathrm{Aa}}, F_{\mathrm{AA}})$, is a vector containing the random variables for the numbers of females of each genotype the mutant male mates (e.g., F_{aa} is a random variable for the number of aa females he mates).

By definition, M has support $\{0, 1, \ldots, N/2\}$, and if male competitiveness follows a Beta distribution with parameters α and $\beta = \alpha(N/2-1)$ (such that $C_i \sim \mathrm{B}(\alpha, \alpha(N/2-1))$ where C_i is the random variable for competitiveness for each male i), then

$$M \sim \mathrm{BetaBin}\left(N/2, \alpha, \beta\right) \tag{B-9}$$

where BetaBin refers to the Beta-binomial distribution (Lee et al., 2008, eq. 1 with their n_i large). The random-variable M has expectation $\mathrm{E}[M] = 1$ and variance $\mathrm{Var}[M] = (N-2)(1+\alpha)/(2+N\alpha) \to 1 + 1/\alpha$ as $N \to \infty$. The parameter α therefore scales the variance in male mating success (through its effect on the distribution of male competitiveness), which is high when α is small and low when α is large.

Because mating is random with respect to genotype, the number of females of each genotype (AA, Aa,

and aa) that the mutant male mates with, given he mates a total m females follows a Multinomial law with parameters

$$\boldsymbol{F}|M = m \sim \text{Multinomial}\,(m, \boldsymbol{\pi}) \tag{B-10}$$

where $\boldsymbol{\pi} = \left((1-\widehat{p}_{\mathrm{f}})(1-\widehat{p}^{\mathrm{X}}_{\mathrm{m}})\frac{w_{\mathrm{f}}(z_{\mathrm{aa}})}{\overline{w}_{\mathrm{f}}}, \left(\widehat{p}_{\mathrm{f}}(1-\widehat{p}^{\mathrm{X}}_{\mathrm{m}}) + (1-\widehat{p}_{\mathrm{f}})\widehat{p}^{\mathrm{X}}_{\mathrm{m}}\right)\frac{w_{\mathrm{f}}(z_{\mathrm{Aa}})}{\overline{w}_{\mathrm{f}}}, \widehat{p}_{\mathrm{f}}\widehat{p}^{\mathrm{X}}_{\mathrm{m}}\frac{w_{\mathrm{f}}(z_{\mathrm{AA}})}{\overline{w}_{\mathrm{f}}}\right)$ gives the frequencies of each genotype amongst adult females. We have denoted the support of this random variable as $\mathscr{F} = \{\boldsymbol{f} = (f_{\mathrm{aa}}, f_{\mathrm{Aa}}, f_{\mathrm{AA}}) : \boldsymbol{f} \in \mathbb{Z}^3_{\geq 0}, f_{\mathrm{aa}} + f_{\mathrm{Aa}} + f_{\mathrm{AA}} = m\}$.

Finally, given it mates with a group of $\boldsymbol{f} = (f_{\mathrm{aa}}, f_{\mathrm{Aa}}, f_{\mathrm{AA}})$ females, the number of surviving male offspring a mutant male sires (the random variable X) is the sum of all the surviving sons of these females. According to our lifecycle (whereby females each produce a large number of juveniles that each compete independently and sex-specifically to obtain a breeding spot), the numbers of surviving male offspring of each genotype produced by a given female follow poisson distributions with means equal to the relative male fitness of each genotype weighted by the proportion of the focal female's juvenile offspring that will carry each genotype. For example, a female with genotype Aa mated to a male carrying A on his Y-chromosome will produce AA and Aa juvenile sons in equal proportions, and so will leave Poisson distributed numbers of surviving male AA and Aa offspring with means $\frac{1}{2}\frac{w_{\mathrm{m}}(2x_{\mathrm{A}})}{\overline{w}_{\mathrm{m}}}$ and $\frac{1}{2}\frac{w_{\mathrm{m}}(x_{\mathrm{a}}+x_{\mathrm{A}})}{\overline{w}_{\mathrm{m}}}$, respectively. Putting all this together, we have

$$X|\boldsymbol{F} = \boldsymbol{f} \sim \text{Poisson}\left(\frac{w_{\mathrm{m}}(x_{\mathrm{a}} + x_{\mathrm{A}})}{\overline{w}_{\mathrm{m}}}(f_{\mathrm{aa}} + f_{\mathrm{Aa}}/2) + \frac{w_{\mathrm{m}}(2x_{\mathrm{A}})}{\overline{w}_{\mathrm{m}}}(f_{\mathrm{AA}} + f_{\mathrm{Aa}}/2)\right). \tag{B-11}$$

Using eqs. (B-9)-(B-11) for eq. (B-8) then gives us the unconditional probability mass function $\Pr(X = j)$.

To generate main text Fig. 3C we plugged eq. (B-8) into eq. (B-4) and solved numerically for $\Psi^{\mathrm{Y}}_{\mathrm{A}}$, doing this for different values of α that lead to different mating variances. For computational expediency we performed the calculation with small population sizes; $N = 20$ when $\alpha \geq 1$ and $N = 100$ otherwise, but which were nonetheless sufficient to capture full probability distribution of M, i.e., $\Pr(M \leq 10) \approx 1$ when $\alpha \geq 1$ and $\Pr(M \leq 50) \approx 1$ for all other values of α considered, so that this procedure was not problematic given our broader assumption that N is large. We calculated substitution times in the same way as for the random-union-of-gametes model (described in Appendix B.2.2) to produce Fig. 3D.

In addition, we ran individual-based simulations for the fixation of a recombination suppressor under lottery polyny to compare with our numerical results for Ψ^{Y}. To apply the polygyny lifecycle, we modelled a population of fixed size N with $N/2$ male and female adults with the following stages:

Each generation, adult females independently sample a mate (i.e., males are sampled with replacement) to sire all her offspring. A males' sampling probability was weighted by his competitiveness, drawn from a Beta distribution. Females then each produce 20 juveniles. Adults die and juveniles $N/2$ juvenile males and $N/2$ juvenile females are sampled (without replacement) to become the adults of the next generation, while all other juveniles die. A male juvenile's sampling probability was weighted by $w_{\mathrm{m}}(z)$ and a female juvenile's by $w_{\mathrm{f}}(z)$. Following the same simulations procedure as in Appendix B.2.2, we computed proportion of simulations in which a novel suppressor fixed when introduced as a single copy, and found a good match with the unconditional invasion probability, Ψ^{Y}, calculated using eq. (B-8) (see dots in Fig. 3C).

C Evolution of an X-linked suppressor

C.1 Invasion fitness

In this Appendix we consider the fate of a new modifier on the X-chromosome that arises in the SDR-homologue and suppresses recombination with the trait locus in male or female heterozygotes for the modifier (as per a chromosomal inversion). Because a new X-linked suppressor may arise in either a male or a female chromosome, we compute its invasion fitness, $W^{\mathrm{X}}_{r,u}(x_{\mathrm{a}}, x_{\mathrm{A}})$, conditional on capturing allele $u \in \{\mathrm{a}, \mathrm{A}\}$, as the leading eigenvalue of the mean matrix

$$\mathrm{M}_{r,u}(x_{\mathrm{a}}, x_{\mathrm{A}}) = \begin{pmatrix} W^{\mathrm{f}\to\mathrm{f}}_{r,u}(x_{\mathrm{a}}, x_{\mathrm{A}}) & W^{\mathrm{m}\to\mathrm{f}}_{r,u}(x_{\mathrm{a}}, x_{\mathrm{A}}) \\ W^{\mathrm{f}\to\mathrm{m}}_{r,u}(x_{\mathrm{a}}, x_{\mathrm{A}}) & W^{\mathrm{m}\to\mathrm{m}}_{r,u}(x_{\mathrm{a}}, x_{\mathrm{A}}) \end{pmatrix}, \tag{C-1}$$

where $W^{i\to j}_{r,u}(x_{\mathrm{a}}, x_{\mathrm{A}})$ gives the number of recruited gametes of sex $j \in \{\mathrm{f}, \mathrm{m}\}$ (i.e., number of sperm and number of eggs, respectively) containing allele $u \in \{\mathrm{a}, \mathrm{A}\}$ produced over the course of a generation by a recruited gamete of sex $i \in \{\mathrm{f}, \mathrm{m}\}$ and carrying allele $u \in \{\mathrm{a}, \mathrm{A}\}$. These fitness components are:

$$\begin{aligned}
W^{\mathrm{f}\to\mathrm{f}}_{r,u}(x_{\mathrm{a}}, x_{\mathrm{A}}) &= \frac{1}{2}\left(\frac{w_{\mathrm{f}}(x_{\mathrm{a}} + x_u)}{\overline{w}_{\mathrm{f}}}\left(1 - \widehat{p}^{\mathrm{m}}_{\mathrm{m}}\right) + \frac{w_{\mathrm{f}}(x_{\mathrm{A}} + x_u)}{\overline{w}_{\mathrm{f}}}\widehat{p}^{\mathrm{X}}_{\mathrm{m}}\right) \\
W^{\mathrm{m}\to\mathrm{f}}_{r,u}(x_{\mathrm{a}}, x_{\mathrm{A}}) &= \frac{w_{\mathrm{f}}(x_{\mathrm{a}} + x_u)}{\overline{w}_{\mathrm{f}}}\left(1 - \widehat{p}_{\mathrm{f}}\right) + \frac{w_{\mathrm{f}}(x_{\mathrm{A}} + x_u)}{\overline{w}_{\mathrm{f}}}\widehat{p}_{\mathrm{f}} \\
W^{\mathrm{f}\to\mathrm{m}}_{r,u}(x_{\mathrm{a}}, x_{\mathrm{A}}) &= \frac{1}{2}\left(\frac{w_{\mathrm{m}}(x_{\mathrm{a}} + x_u)}{\overline{w}_{\mathrm{m}}}\left(1 - \widehat{p}^{\mathrm{Y}}_{\mathrm{m}}\right) + \frac{w_{\mathrm{m}}(x_{\mathrm{A}} + x_u)}{\overline{w}_{\mathrm{m}}}\widehat{p}^{\mathrm{Y}}_{\mathrm{m}}\right) \\
W^{\mathrm{m}\to\mathrm{m}}_{r,u}(x_{\mathrm{a}}, x_{\mathrm{A}}) &= 0.
\end{aligned} \tag{C-2}$$

where $\overline{w}_{\mathrm{m}}$ and $\overline{w}_{\mathrm{f}}$ are given by eq. (A-6).

The quantities $W^{\mathrm{X}}_{r,\mathrm{A}}(x_{\mathrm{a}}, x_{\mathrm{A}})$ and $W^{\mathrm{X}}_{r,\mathrm{a}}(x_{\mathrm{a}}, x_{\mathrm{A}})$ end up being cumbersome, and so are given in a Supplementary Mathematica Notebook. They also do not lead to readily interpretable invasion conditions ($W^{\mathrm{Y}}_{r,\mathrm{A}}(x_{\mathrm{a}}, x_{\mathrm{A}}) > 1$ and $W^{\mathrm{Y}}_{r,\mathrm{a}}(x_{\mathrm{a}}, x_{\mathrm{A}}) > 1$) for an X-linked modifier, so we again proceed with a numerical analysis. Using Gaussian functions for $w_{\mathrm{f}}(z)$ and $w_{\mathrm{m}}(z)$ and following an identical procedure as in Appendix B.1, we find that across all parameter $(\sigma_{\mathrm{m}}, \sigma_{\mathrm{f}}, r)$ and allelic value $(x_{\mathrm{a}}, x_{\mathrm{A}})$ combinations tested, an X-linked suppressor invades only when it captures the female-beneficial allele a, and is otherwise disfavoured by selection (i.e., $W^{\mathrm{X}}_{r,\mathrm{A}}(x_{\mathrm{a}}, x_{\mathrm{A}}) < 1$ and $W^{\mathrm{X}}_{r,\mathrm{a}}(x_{\mathrm{a}}, x_{\mathrm{A}}) > 1$ for all $x_{\mathrm{a}}, x_{\mathrm{A}}, \sigma_{\mathrm{m}}, \sigma_{\mathrm{f}}$ and r). We therefore drop the dependency of invasion fitness (and its components) on allele u, and use the notation $W^{\mathrm{X}}_{r}(x_{\mathrm{a}}, x_{\mathrm{A}}) = W^{\mathrm{X}}_{r,\mathrm{a}}(x_{\mathrm{a}}, x_{\mathrm{A}})$ in the main text (e.g., in section 3.4) and for the rest of the Appendix. We present plots of $W^{\mathrm{X}}_{r}(x_{\mathrm{a}}, x_{\mathrm{A}})$ for different allelic values and parameters in SI Fig. 4 (calculated with the same procedure as Appendix B.1), and the strength of selection for a Y-suppressor relative to an X-suppressor ($W^{\mathrm{Y}}_{r}(x_{\mathrm{a}}, x_{\mathrm{A}}) / W^{\mathrm{X}}_{r}(x_{\mathrm{a}}, x_{\mathrm{A}})$) in SI Fig. 5A.

C.2 Invasion and fixation probabilities for X-linked suppressors based on multitype branching process

C.2.1 Probability of invasion

As an X-linked suppressor can only be favoured by selection when it captures allele a, its unconditional probability of invasion, Ψ^{X}, depends on its probabilities of invasion conditional on the mutant arising on a male, $\Psi^{\mathrm{X}}_{\mathrm{m}}$, and female, $\Psi^{\mathrm{X}}_{\mathrm{f}}$, X-chromosome carrying allele a, weighted by the equilibrium frequencies of this allele; $1 - \widehat{p}_{\mathrm{f}}$ and $1 - \widehat{p}^{\mathrm{X}}_{\mathrm{m}}$. Specifically, taking into account the difference in male and female X copy numbers (and so likelihood of a given X-linked mutation first appearing in a male or female), we have

$$\Psi^{\mathrm{X}} = \frac{2}{3}(1 - \widehat{p}_{\mathrm{f}})\Psi^{\mathrm{X}}_{\mathrm{f}} + \frac{1}{3}(1 - \widehat{p}^{\mathrm{X}}_{\mathrm{m}})\Psi^{\mathrm{X}}_{\mathrm{m}} \tag{C-3}$$

(Charlesworth et al., 1987).

The growth of the mutant suppressor arisen as a single copy follows a multitype branching process (Harris et al., 1963). As such, if a rare mutant can invade into a population (i.e., if $W^{\mathrm{X}}_{r}(x_{\mathrm{a}}, x_{\mathrm{A}}) > 1$), the probability this mutant ultimately invades conditional on it arising in a gamete produced by sex $i \in \{\mathrm{f}, \mathrm{m}\}$ is Ψ^{X}_{i}. If mutant fitness distributions are Poisson for all genetic backgrounds, that is, if $X^{i\to j} \sim \mathrm{Pois}\left(W^{i\to j}_{r,\mathrm{a}}(x_{\mathrm{a}}, x_{\mathrm{A}})\right)$ for all $i \in \{\mathrm{f}, \mathrm{m}\}$ and $j \in \{\mathrm{f}, \mathrm{m}\}$, where $X^{i\to j}$ is the random variable for the number of mutants in a gamete of sex j produced by a mutant in gamete of sex i, then $\boldsymbol{\Psi}^{\mathrm{X}} = (\Psi^{\mathrm{X}}_{\mathrm{f}}, \Psi^{\mathrm{X}}_{\mathrm{m}})$ is the

unique solution to the set of simultaneous equations

$$\begin{aligned} 1-\Psi_{\mathrm{f}}^{\mathrm{X}} &= \exp\left(-W_r^{\mathrm{f}\to\mathrm{f}}(x_{\mathrm{a}},x_{\mathrm{A}})\Psi_{\mathrm{f}}^{\mathrm{X}} - W_r^{\mathrm{f}\to\mathrm{m}}(x_{\mathrm{a}},x_{\mathrm{A}})\Psi_{\mathrm{m}}^{\mathrm{X}}\right) \\ 1-\Psi_{\mathrm{m}}^{\mathrm{X}} &= \exp\left(-W_r^{\mathrm{m}\to\mathrm{f}}(x_{\mathrm{a}},x_{\mathrm{A}})\Psi_{\mathrm{f}}^{\mathrm{X}} - W_r^{\mathrm{m}\to\mathrm{m}}(x_{\mathrm{a}},x_{\mathrm{A}})\Psi_{\mathrm{m}}^{\mathrm{X}}\right) \end{aligned} \tag{C-4}$$

(where recall $W_r^{i\to j}(x_{\mathrm{a}},x_{\mathrm{A}})$ refers to $W_{r,\mathrm{a}}^{i\to j}(x_{\mathrm{a}},x_{\mathrm{A}})$ in eq. C-2). Taking the log of both sides of eq. (C-4) and rearranging, we arrive at the system

$$\begin{aligned} -\mathrm{Log}(1-\Psi_{\mathrm{f}}^{\mathrm{X}}) &= W_r^{\mathrm{f}\to\mathrm{f}}(x_{\mathrm{a}},x_{\mathrm{A}})\Psi_{\mathrm{f}}^{\mathrm{X}} + W_r^{\mathrm{f}\to\mathrm{m}}(x_{\mathrm{a}},x_{\mathrm{A}})\Psi_{\mathrm{m}}^{\mathrm{X}} \\ -\mathrm{Log}(1-\Psi_{\mathrm{m}}^{\mathrm{X}}) &= W_r^{\mathrm{m}\to\mathrm{f}}(x_{\mathrm{a}},x_{\mathrm{A}})\Psi_{\mathrm{f}}^{\mathrm{X}} + W_r^{\mathrm{m}\to\mathrm{m}}(x_{\mathrm{a}},x_{\mathrm{A}})\Psi_{\mathrm{m}}^{\mathrm{X}}. \end{aligned} \tag{C-5}$$

After plugging in eq. (C-2), eq. (C-5) can be solved numerically for $\Psi_{\mathrm{m}}^{\mathrm{X}}$ and $\Psi_{\mathrm{f}}^{\mathrm{X}}$ using the same approach as we used to find Ψ^{Y} in Appendix B.2.1. Finally, plugging these quantities into eq. (C-3) with the corresponding equilibrium frequencies $\hat{p}_{\mathrm{f}}$ and $\hat{p}_{\mathrm{m}}^{\mathrm{X}}$ allowed and comparing with the equivalent invasion probabilities for Y-linked suppressors (to calculate $\Psi^{\mathrm{Y}}/\Psi^{\mathrm{X}}$ and $\rho = \Psi^{\mathrm{Y}}/(\Psi^{\mathrm{Y}}+\Psi^{\mathrm{X}})$), we could produce Fig. 4A and SI Fig. 5B.

C.2.2 Fixation and substitution

In order to confirm that successfully invading X-linked suppressors also go on to fix, we ran individual-based simulations following the same procedure as in Appendix B.2.2. Depending on the scenario being considered, we either introduced a suppressor (1) as a single copy into the population, by placing it in a randomly sampled X-chromosome (which could be present in an adult male or female; example frequency trajectories are shown in Appendix Fig. 1B), or (2) at a frequency $q = 1/(3N/4\Psi^{\mathrm{X}})$ by adding it to $3Nq/4$ (again rounded to the nearest integer) randomly sampled a-bearing X-chromosomes. Across the same parameter sets as used in Appendix B.2.2, we found that when introduced at frequency q, X-linked suppressors always went on to fix in the population. Furthermore, for simulations where the suppressor was introduced as a single copy, we saw a good match between the proportion of replicates in which this mutant fixed and our numerical calculation of Ψ^{X} in Appendix C.2.1 (see dots in Appendix Fig 2). This is consistent with invasion implying fixation for X-linked suppressors and we therefore interpret Ψ^{X} as both the probability of invasion and fixation.

In contrast to these results, Olito and Abbott (2023) (see their Appendix C and Fig. S5) report that invading X-linked inversions capturing the SDR-homologue and the female-beneficial allele at a sex-

ually antagonistic locus do not fix, but instead reach a stable polymorphism maintained by negative frequency-dependent selection. Based on the low equilibrium frequencies they observe (typically < 0.2; Olito and Abbott, 2023, Fig. S5 C-D), the authors argue that such suppressors are likely to be lost over time and thus unlikely to contribute meaningfully to the evolution of recombination suppression. These findings were obtained using deterministic population genetic recursions, but we have not been able to reproduce them using our approach (see above) even though the underlying biological assumptions appear to be the same. It is also unclear to us what biological process would lead selection on an X-linked suppressor under these assumptions, and no explanation is provided in Olito and Abbott (2023). Furthermore, Olito and Abbott (2023) present an expression for the invasion fitness of an X-linked modifier (their Appendix eq. 26) that differs from the one we obtain from the mean matrix eq. (C-1). When evaluated under the same fecundity functions (Gaussian functions), their expression gives substantially larger values than ours that would be totally inconsistent with the probabilities of invasion than we see in our individual-based simulations (whereas we observe a good fit with simulations, compare line and dots in Appendix Fig 2). We are currently in contact with the authors in an effort to clarify the origin of these discrepancies.

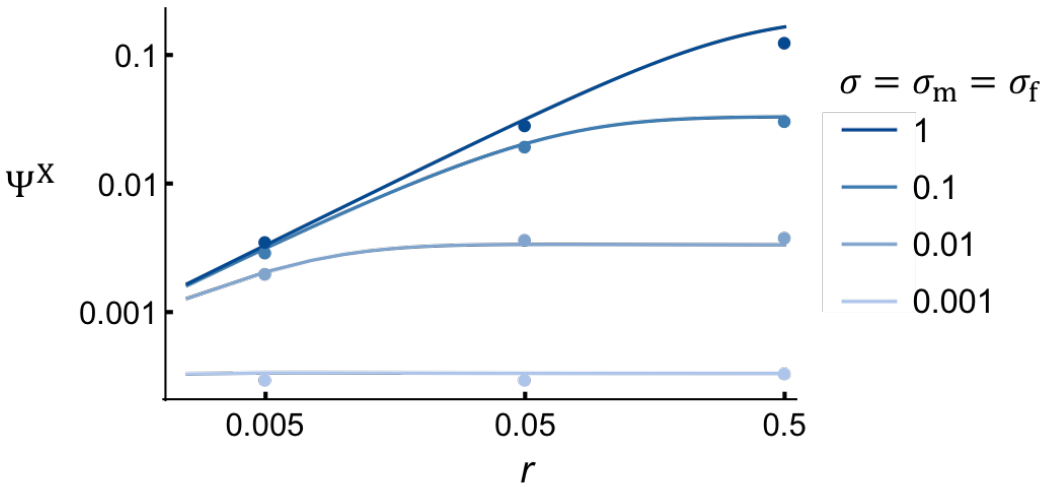

Appendix Figure 2: **Invasion of X-linked suppressors in a large population**. Figure shows the unconditional invasion probability of a newly arisen X-linked suppressor in a large population, Ψ^X, under the random-union-of-gametes model (Appendix C.2.1 for calculation) according to the resident recombination rate (r). Allelic values used: $x_a = 0.5$ and $x_A = -0.5$. Dots show results from individual-based simulations with (which correspond to proportion of replicate simulations in which a X-suppressor fixed, Appendix C.2.2). Different colour curves and dots correspond to results for different strengths of sexually antagonistic selection at the trait locus ($\sigma = \sigma_m = \sigma_f$).

C.3 Invasion of X-suppressors under polygyny

Calculating the invasion probability of an X-linked suppressor from a multitype branching process in the presence of lottery polygyny is complex, as it involves considering male and female fitness distributions (the latter of which depend on the distribution of mating success across males). We therefore estimated its fixation probability directly using individual-based simulations. This involved an identical simulation procedure as described in Appendix B.2.3, except that here a recombination suppressor was introduced as a single copy into a randomly sampled X-chromosome (rather than Y-chromosome). We then calculated the fixation probability for a given parameter set as the proportion of replicates in which the suppressor fixed. We used this proportion in place of Ψ^{X} when producing Fig. 4B.

D Simulating polygenic variation on the PAR

In this Appendix, we investigate whether male heterozygote advantage evolves in response to sexually antagonistic selection (as found under the continuum-of-alleles model, Appendix A) when z shows a polygenic basis on the PAR. To do this, we ran simulations where z was encoded by 10 di-allelic quantitative trait loci (with additive effects on the phenotypes) under the random-union-of-gametes model (Appendix B.2.1 for implementation of this lifecycle in a simulation). At each locus one segregating allele encodes an effect 0.25 and the other −0.25; these values were chosen for illustrative purposes, as they allow for a wide range of haplotype values, including the common evolutionarily stable coalition in the continuum-of-alleles-model ($x_a^* \approx 0.5, x_A^* \approx -1.5$). We assumed loci were equally spaced along the PAR with a uniform recombination rate r (i.e., r is the probability of recombination between adjacent trait loci, and between the SDR and the closest terminal trait locus) and we initialised simulations with equal frequencies of each allele at each locus. We tracked the evolution of the genetic values encoded by X and Y chromosomes over 15000 generations of sexually antagonistic selection (under Gaussian fecundity functions with $\sigma = 0.1$ for illustration). Results are shown in Appendix Fig. 3.

With strong recombination (e.g., $r/\sigma = 0.5$), genetic values for the X and Y evolve to be distributed symmetrically around 0 (similar to autosomal chromosome pairs, Flintham et al., 2024), however, where recombination is weaker (e.g., $r/\sigma = 0.1$ or $r/\sigma = 0.05$), X-chromosome haplotypes develop that tend to encode an allelic value of 0.5 or smaller, while Y-chromosome haplotypes encode a much

larger absolute effect that overshoots the male optimum in homozygous state. Indeed when linkage is tight, e.g., $r/\sigma = 0.01$, haplotype values are distributed around the evolutionary stable coalition (i.e., X-haplotype encoding $x_a^* = 0.5$ and Y-linked haplotype encoding $x_A^* = -1.5$). Consequently, when z shows a polygenic basis that is in linkage with the SDR (i.e., in the PAR), we expect that females show highest fitness when homozygous for the most common X-linked haplotype, and so are homozygotes across trait loci. Meanwhile, the highest fitness males, that is, those carrying one copy of the most common Y- and X- haplotypes, are heterozygous across loci, leading to heterozygote advantage.

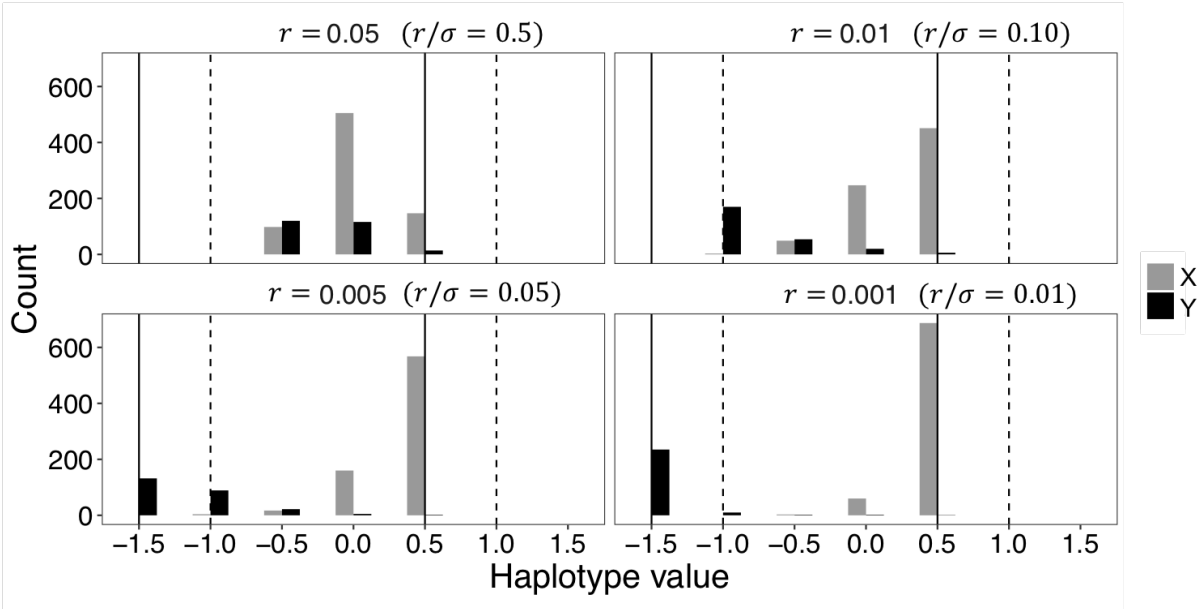

Appendix Figure 3: **Evolved haplotypes when z is polygenic**. Panels show distributions of genetic effects encoded by a sample of 1000 chromosomes (grey and black columns for X and Y chromosomes, respectively) segregating in the population after 15000 generations of a simulation. Different panels show results for different strengths of recombination amongst loci, r. Vertical dotted lines indicate the location of the male and female optima (at −1 and 1, respectively) and vertical solid lines indicate the evolutionary stable allelic values ($x_A^* \approx -1.5$ and $x_a^* \approx 0.5$, see Fig. 1C).

References

Andersson, M. B. (1994). *Sexual selection*. Princeton University Press.

Avila, P. and Mullon, C. (2023). Evolutionary game theory and the adaptive dynamics approach: adaptation where individuals interact. *Philosophical Transactions of the Royal Society B*, 378(1876):20210502.

Bachtrog, D. (2013). Y-chromosome evolution: emerging insights into processes of y-chromosome degeneration. *Nature Reviews Genetics*, 14(2):113–124.

Bachtrog, D., Mank, J. E., Peichel, C. L., Kirkpatrick, M., Otto, S. P., Ashman, T.-L., Hahn, M. W., Kitano, J., Mayrose, I., Ming, R., et al. (2014). Sex determination: why so many ways of doing it? *PLoS biology*, 12(7):e1001899.

Berdan, E. L., Barton, N. H., Butlin, R., Charlesworth, B., Faria, R., Fragata, I., Gilbert, K. J., Jay, P., Kapun, M., Lotterhos, K. E., et al. (2023). How chromosomal inversions reorient the evolutionary process. *Journal of Evolutionary Biology*, 36(12):1761–1782.

Berdan, E. L., Blanckaert, A., Slotte, T., Suh, A., Westram, A. M., and Fragata, I. (2021). Unboxing mutations: Connecting mutation types with evolutionary consequences. *Molecular Ecology*, 30(12):2710–2723.

Bergero, R. and Charlesworth, D. (2009). The evolution of restricted recombination in sex chromosomes. *Trends in ecology & evolution*, 24(2):94–102.

Beukeboom, L. W. and Perrin, N. (2014). *The evolution of sex determination*. Oxford University Press.

Blaser, O., Grossen, C., Neuenschwander, S., and Perrin, N. (2013). Sex-chromosome turnovers induced by deleterious mutation load. *Evolution*, 67(3):635–645.

Blaser, O., Neuenschwander, S., and Perrin, N. (2014). Sex-chromosome turnovers: the hot-potato model. *The American Naturalist*, 183(1):140–146.

Bonduriansky, R. and Chenoweth, S. F. (2009). Intralocus sexual conflict. *Trends in ecology & evolution*, 24(5):280–288.

Charlesworth, B. (2020). How long does it take to fix a favorable mutation, and why should we care? *The American Naturalist*, 195(5):753–771.

Charlesworth, B., Coyne, J. A., and Barton, N. H. (1987). The relative rates of evolution of sex chromosomes and autosomes. *The American Naturalist*, 130(1):113–146.

Charlesworth, B., Jordan, C. Y., and Charlesworth, D. (2014). The evolutionary dynamics of sexually antagonistic mutations in pseudoautosomal regions of sex chromosomes. *Evolution*, 68(5):1339–1350.

Charlesworth, B. and Olito, C. (2024). Making sense of recent models of the "sheltering" hypothesis for recombination arrest between sex chromosomes. *Evolution*, page qpae119.

Charlesworth, D. and Charlesworth, B. (1980). Sex differences in fitness and selection for centric fusions between sex-chromosomes and autosomes. *Genetics Research*, 35(2):205–214.

Charlesworth, D. and Charlesworth, B. (2005). Steps in the evolution of heteromorphic sex chromosomes. *Heredity*, 95(2):118–128.

Clark, A. (1988). The evolution of the y chromosome with xy recombination. *Genetics*, 119(3):711–720.

Clutton-Brock, T. H. and Parker, G. A. (1992). Potential reproductive rates and the operation of sexual selection. *The Quarterly Review of Biology*, 67(4):437–456.

Connallon, T. and Clark, A. G. (2014a). Balancing selection in species with separate sexes: insights from fisher's geometric model. *Genetics*, 197(3):991–1006.

Connallon, T. and Clark, A. G. (2014b). Evolutionary inevitability of sexual antagonism. *Proceedings of the Royal Society B: Biological Sciences*, 281(1776):20132123.

Dercole, F. and Rinaldi, S. (2008). *Analysis of evolutionary processes*. Princeton University Press.

Fisher, R. A. (1931). The evolution of dominance. *Biological Reviews of the Cambridge Philosophical Society*, 6(4):345–368.

Fisher, R. A. (1958). *The genetical theory of natural selection*. Oxford University Press.

Flintham, E., Savolainen, V., Otto, S., Reuter, M., and Mullon, C. (2024). The maintenance of genetic polymorphism in sexually antagonistic traits. *bioRxiv*.

Geritz, S. A. and Kisdi, É. (2000). Adaptive dynamics in diploid, sexual populations and the evolution of reproductive isolation. *Proceedings of the Royal Society of London. Series B: Biological Sciences*, 267(1453):1671–1678.

Geritz, S. A., Kisdi, E., Metz, J. A., et al. (1998). Evolutionarily singular strategies and the adaptive growth and branching of the evolutionary tree. *Evolutionary ecology*, 12(1):35–57.

Haldane, J. (1962). Conditions for stable polymorphism at an autosomal locus. *Nature*, 193(4820):1108–1108.

Haldane, J. B. S. (1927). A mathematical theory of natural and artificial selection, part v: selection and mutation. In *Mathematical Proceedings of the Cambridge Philosophical Society*, volume 23, pages 838–844. Cambridge University Press.

Haller, B. C. and Messer, P. W. (2023). Slim 4: multispecies eco-evolutionary modeling. *The American Naturalist*, 201(5):E127–E139.

Harris, T. E. et al. (1963). *The theory of branching processes*, volume 6. Springer Berlin.

Ironside, J. E. (2010). No amicable divorce? challenging the notion that sexual antagonism drives sex chromosome evolution. *BioEssays*, 32(8):718–726.

Janicke, T., Häderer, I. K., Lajeunesse, M. J., and Anthes, N. (2016). Darwinian sex roles confirmed across the animal kingdom. *Science advances*, 2(2):e1500983.

Jay, P., Jeffries, D., Hartmann, F. E., Véber, A., and Giraud, T. (2024). Why do sex chromosomes progressively lose recombination? *Trends in Genetics*.

Jay, P., Tezenas, E., Véber, A., and Giraud, T. (2022). Sheltering of deleterious mutations explains the stepwise extension of recombination suppression on sex chromosomes and other supergenes. *PLoS biology*, 20(7):e3001698.

Jordan, C. Y. and Charlesworth, D. (2012). The potential for sexually antagonistic polymorphism in different genome regions. *Evolution: International Journal of Organic Evolution*, 66(2):505–516.

Kidwell, J., Clegg, M., Stewart, F., and Prout, T. (1977). Regions of stable equilibria for models of differential selection in the two sexes under random mating. *Genetics*, 85(1):171–183.

Kimura, M. (1965). A stochastic model concerning the maintenance of genetic variability in quantitative characters. *Proceedings of the National Academy of Sciences*, 54(3):731–736.

Kirkpatrick, M. (2010). How and why chromosome inversions evolve. *PLoS biology*, 8(9):e1000501.

Lande, R. (1980). Sexual dimorphism, sexual selection, and adaptation in polygenic characters. *Evolution*, 34(2):292–305.

Laporte, V. and Charlesworth, B. (2002). Effective population size and population subdivision in demographically structured populations. *Genetics*, 162(1):501–519.

Lee, A. M., Engen, S., and Sæther, B.-E. (2008). Understanding mating systems: a mathematical model of the pair formation process. *Theoretical Population Biology*, 73(1):112–124.

Lehtonen, J. (2022). Bateman gradients from first principles. *Nature Communications*, 13(1):3591.

Lenormand, T. (2003). The evolution of sex dimorphism in recombination. *Genetics*, 163(2):811–822.

Lenormand, T. and Roze, D. (2022). Y recombination arrest and degeneration in the absence of sexual dimorphism. *Science*, 375(6581):663–666.

Lenormand, T. and Roze, D. (2024). Can mechanistic constraints on recombination reestablishment explain the long-term maintenance of degenerate sex chromosomes? *Peer Community Journal*, 4.

Liu, Z., Herbert, A. L., Chan, Y. F., Kučka, M., Kingsley, D. M., and Peichel, C. L. (2025). The fourspine stickleback (apeltes quadracus) has an xy sex chromosome system with polymorphic inversions on both x and y chromosomes. *PLoS genetics*, 21(5):e1011465.

Maynard Smith, J. (1976). What determines the rate of evolution? *The American Naturalist*, 110(973):331–338.

McAllister, B. F. (2003). Sequence differentiation associated with an inversion on the neo-x chromosome of drosophila americana. *Genetics*, 165(3):1317–1328.

Muralidhar, P. and Coop, G. (2023). Polygenic outcomes of sexually antagonistic selection. *bioRxiv*, pages 2023–03.

Nei, M. (1969). Linkage modification and sex difference in recombination. *Genetics*, 63(3):681.

Nunney, L. (1993). The influence of mating system and overlapping generations on effective population size. *Evolution*, 47(5):1329–1341.

Olito, C. and Abbott, J. K. (2023). The evolution of suppressed recombination between sex chromosomes and the lengths of evolutionary strata. *Evolution*, 77(4):1077–1090.

Olito, C., Ponnikas, S., Hansson, B., and Abbott, J. K. (2024). Consequences of partially recessive deleterious genetic variation for the evolution of inversions suppressing recombination between sex chromosomes. *Evolution*, 78(8):1499–1510.

Otto, S. P. (2014). Selective maintenance of recombination between the sex chromosomes. *Journal of Evolutionary Biology*, 27(7):1431–1442.

Otto, S. P. and Day, T. (2011). *A Biologist's Guide to Mathematical Modeling in Ecology and Evolution*. Princeton University Press.

Otto, S. P., Pannell, J. R., Peichel, C. L., Ashman, T.-L., Charlesworth, D., Chippindale, A. K., Delph, L. F., Guerrero, R. F., Scarpino, S. V., and McAllister, B. F. (2011). About par: the distinct evolutionary dynamics of the pseudoautosomal region. *Trends in Genetics*, 27(9):358–367.

Otto, S. P. and Whitlock, M. C. (2001). Fixation probabilities and times. *e LS*.

Pokorna, M. and Kratochvíl, L. (2009). Phylogeny of sex-determining mechanisms in squamate reptiles: are sex chromosomes an evolutionary trap? *Zoological Journal of the Linnean Society*, 156(1):168–183.

Ponnikas, S., Sigeman, H., Abbott, J. K., and Hansson, B. (2018). Why do sex chromosomes stop recombining? *Trends in Genetics*, 34(7):492–503.

Rice, W. R. (1984). Sex chromosomes and the evolution of sexual dimorphism. *Evolution*, 38(4):735–742.

Rueffler, C., Van Dooren, T. J., Leimar, O., and Abrams, P. A. (2006). Disruptive selection and then what? *Trends in Ecology & Evolution*, 21(5):238–245.

Shuker, D. M. and Simmons, L. W. (2014). *The evolution of insect mating systems*. Number 27. Oxford University Press, USA.

Vicoso, B. (2019). Molecular and evolutionary dynamics of animal sex-chromosome turnover. *Nature ecology & evolution*, 3(12):1632–1641.

Wade, M. J. and Shuster, S. M. (2004). Sexual selection: harem size and the variance in male reproductive success. *The American Naturalist*, 164(4):E83–E89.

Wilson, A. J. and Nussey, D. H. (2010). What is individual quality? an evolutionary perspective. *Trends in ecology & evolution*, 25(4):207–214.

Wright, A. E., Dean, R., Zimmer, F., and Mank, J. E. (2016). How to make a sex chromosome. *Nature communications*, 7(1):12087.

Yue, J., Krasovec, M., Kazama, Y., Zhang, X., Xie, W., Zhang, S., Xu, X., Kan, B., Ming, R., and Filatov, D. A. (2023). The origin and evolution of sex chromosomes, revealed by sequencing of the silene latifolia female genome. *Current Biology*, 33(12):2504–2514.

Zhou, Q., Zhang, J., Bachtrog, D., An, N., Huang, Q., Jarvis, E. D., Gilbert, M. T. P., and Zhang, G. (2014). Complex evolutionary trajectories of sex chromosomes across bird taxa. *Science*, 346(6215):1246338.